Vol. 720: 1–24, 2023
https://doi.org/10.3354/meps14396

MARINE ECOLOGY PROGRESS SERIES
Mar Ecol Prog Ser

Published October 5

FEATURE ARTICLE

Spatial and temporal separation of toothed whales in the western North Atlantic

Rebecca E. Cohen[1,2,*], Kaitlin E. Frasier[1], Simone Baumann-Pickering[1], John A. Hildebrand[1]

[1]Scripps Institution of Oceanography, University of California San Diego, La Jolla, California 92093, USA
[2]*Present address:* K. Lisa Yang Center for Conservation Bioacoustics, Cornell Lab of Ornithology, Cornell University, Ithaca, New York 14850, USA

ABSTRACT: A diverse group of toothed whale species inhabits the pelagic habitats of the western North Atlantic, competing for overlapping prey resources. Historical data deficits have limited fundamental research into many of these species, such as establishing baselines of distribution and abundance, so their occurrence and habitat use patterns are not well characterized. Periodic cycles in activity have been reported at a range of temporal scales for odontocetes in other regions, such as seasonal movements, foraging activity modulated by lunar cycles, and diel activity patterns. A variety of spatial, temporal, and behavioral separation strategies have also been observed among predator guilds in both marine and terrestrial systems, and these may also contribute to observed spatiotemporal patterns in activity. Recently, passive acoustic data has been applied to monitor odontocete species continuously, with improved detection and species discrimination for some cryptic species. We used a long-term passive acoustic data set collected at sites spanning the western North Atlantic shelf-break region to quantify presence and characterize seasonal, lunar, and diel activity patterns for 10 species. Our results demonstrated strong regional preferences and clear patterns of spatiotemporal separation between species with similar foraging ecology. Latitudinal shifts in seasonal presence peaks may suggest meridional seasonal migrations for some dolphin species. We also observed strong diel activity patterns that were modulated by both seasonal and lunar cycles. This study reveals complex behavioral patterns arising in response to natural cycles playing out over multiple temporal scales and provides new insights into habitat partitioning among toothed whale species.

*Corresponding author: r.cohen@cornell.edu

AI-generated image in response to prompt 'cubist painting of dolphins swimming just under the surface of the water'

Image: Rebecca Cohen x DALL-E

KEY WORDS: Bioacoustics · Odontocetes · Seasonal pattern · Diel rhythms · Lunar cycle · Distributional patterns

1. INTRODUCTION

Effective conservation and management practices rely upon knowledge of species' distributions and habitat use patterns to quantify overlaps with anthropogenic activities. This is especially pertinent for populations that shift their distributions cyclically; for instance, by undergoing seasonal migrations, exposing them to variable anthropogenic impacts in different parts of their habitats. More than 2 dozen odontocete, or toothed whale, species inhabit the pelagic waters of the western North Atlantic, an area heavily subject to anthropogenic activity. Little is known

Publisher: Inter-Research · www.int-res.com

about the habitat use of most of the odontocete species in shelf break and offshore waters of this region, owing to the challenges of observing patchily distributed species with vast oceanic ranges. Such knowledge gaps have limited our basic understanding of these species' life histories and hinder management efforts. The widespread adoption of passive acoustic monitoring over the past several years and the collection of large data sets at offshore monitoring sites means that we are now poised to gain new insights into these difficult-to-access species.

Studies of odontocete populations in several regions have reported distribution and activity patterns modulated at a range of temporal and spatial scales: long-term distribution shifts (Thorne et al. 2022); large-scale movements tracking mesoscale features (Woodworth et al. 2012); seasonal migrations (Taylor et al. 2016); onshore–offshore movements (Gannier 1999); and lunar and diel foraging patterns (Simonis et al. 2017, Cascão et al. 2020). In oceanic food webs, the distribution and activity of highly mobile top predators such as odontocetes are thought to be driven by prey availability (Piatt & Methven 1992, Hastie et al. 2004). The availability of the odontocetes' mid-trophic-level prey is driven by variability in oceanic conditions at a range of temporal and spatial scales: diel vertical migration in response to sunlight and moonlight (Kampa 1975, Last et al. 2016), mesoscale features that can input nutrients, entrap and transport water parcels, and act as particle aggregators (Martin & Richards 2001, Della Penna & Gaube 2020), and seasonal changes in primary and low trophic level productivity in response to differential nutrient and light availability (Legendre 1990, Biktashev et al. 2003). The habitat use patterns of odontocetes in the western North Atlantic likely reflect such patterns in the availability of each species' preferred prey.

Odontocetes exhibit a range of diving behaviors and corresponding prey preferences but can loosely be grouped as 'shallow', 'intermediate', or 'deep' divers. Shallow divers, such as many small-bodied delphinids, feed primarily on epi- and mesopelagic fish and squid when they are accessible in surface waters (Davis et al. 1996). Some of the larger-bodied delphinids, such as Risso's dolphins and pilot whales, exhibit intermediate diving behavior and use specialized deep dives to access mesopelagic prey at greater depth (Aguilar Soto et al. 2008, Quick et al. 2017, Benoit-Bird et al. 2019, Visser et al. 2021). True deep divers, such as beaked whales *Kogia* spp. and sperm whales, are specialized for pursuit of deeper meso-, bathy-, and benthopelagic prey at great depth (Arranz et al. 2011, Barlow et al. 2020, Visser et al. 2022). Species within each of these groups target similar prey, increasing the potential for interspecific competition, but little work has investigated their strategies for subdividing shared habitats. When multiple predator species target shared prey, the predators must maximize foraging efficiency while simultaneously minimizing competitive interactions with other species. A variety of spatial, temporal, and behavioral separation strategies have been observed in such situations that are thought to be means of reducing interspecies competition, such as differing diel activity patterns, depth distributions, seasonal changes in site occupancy or habitat use, and prey specialization (Conners et al. 2015, Matich et al. 2017, Gao et al. 2020, Iwahara et al. 2020, Lear et al. 2021). Observed patterns in odontocete species distribution and activity may therefore reflect not only prey availability but an optimization of foraging efficiency that balances prey availability against the presence of competitors.

The western North Atlantic is characterized by the Gulf Stream current, which bisects the region and acts as a frontal boundary between 2 different oceanic regimes as well as a driver of mixing between very different water masses (Bower et al. 1985). In the offshore region south of Cape Hatteras, North Carolina, warm, high-salinity, low-nutrient Gulf Stream waters originating in the Sargasso Sea dominate the water column. To the north, the primary water masses are all comparatively cool, fresh, and productive, with origins in the subarctic and arising from the mixing of subarctic and Gulf Stream waters (McLellan 1957, Gatien 1976, New et al. 2021). The ecological communities present in these distinct regions delineated by the Gulf Stream front differ substantially (Cavender-Bares et al. 2001, Wang et al. 2018), and thus we might also expect them to be differentially used by top predators.

The spatiotemporal presence and activity patterns of odontocetes in the western North Atlantic have traditionally been estimated by aggregating visual survey data over many years, necessitated by scant sighting records for many species (Hamazaki 2002, Best et al. 2012, Roberts et al. 2016). This approach can provide high-level insights but is confounded by seasonally biased and spatially inconsistent visual survey effort resulting from the expense and logistical challenges of broad-scale shipboard and aerial surveys and their dependence on good sighting conditions (Mellinger et al. 2007). Limited seasonal coverage (i.e. little to no effort in the fall and winter months) means these data are not well-suited to examining seasonal activity patterns across the

entire year, while the sporadic snapshot nature of these surveys means that they are not sensitive to fine-temporal-scale (e.g. weekly, daily, sub-daily) changes in site occupancy or habitat use (Mellinger et al. 2007). Pelagic odontocetes are also difficult to observe due to their vast ranges and at times cryptic behavior, but as highly soniferous species they lend themselves well to acoustic studies. All odontocete species use biosonar for foraging, environmental sensing, and sometimes communication, and, thanks to extensive research and the combination of passive acoustic data with visual surveys, body-mounted tags, focal recordings, and captive studies, these impulsive signals can be readily identified and often classified to the species level in passive acoustic data (Møhl et al. 2000, Marques et al. 2013, Frasier 2021). The increasing popularity of marine passive acoustic monitoring over the past decade has led to the accumulation of large passive acoustic data sets on the order of hundreds of terabytes, with excellent temporal resolution and coverage, and provides the potential for novel insights into the acoustic ecology of many offshore and cryptic species with limited visual observation records (Hildebrand et al. 2015, Campos-Cerqueira & Aide 2016, Gibb et al. 2019, Picciulin et al. 2019, Cohen et al. 2022, Ziegenhorn et al. 2023).

Recent studies have begun to use these rich passive acoustic data sets to address some of the knowledge gaps for odontocetes in the western North Atlantic (Stanistreet et al. 2017, 2018, Hodge et al. 2018, Kowarski et al. 2023). Here, we used the groundwork laid by Cohen et al. (2022), which yielded a high-temporal-resolution time series of labeled odontocete clicks to characterize temporal patterns in acoustic activity for 10 species/groups across a large region at a range of temporal scales. This data set was collected through almost continuous acoustic recording across 3 consecutive years (May 2016–April 2019) at 11 sites arranged across a latitudinal habitat gradient in the western North Atlantic (see Fig. 1). Based on previous findings, we hypothesized that the presence and activity of our species of interest would exhibit some combination of seasonal, lunar, and diel periodicity. To test these hypotheses, we modeled species presence as a response to day-of-year (DOY), moon phase (MPh), and time of day. We also hypothesized that species with similar diving and foraging ecology would mitigate the potential for direct competition through spatiotemporal separation strategies, which we explored by comparing distribution and activity patterns. Here, we report on inter-species, inter-site, and temporal differences in acoustic activity patterns and discuss our findings in light of what is known of each species' foraging ecology and the oceanographic conditions across the study region.

2. MATERIALS AND METHODS

2.1. Acoustic presence data

Time series of labeled odontocete echolocation clicks were derived by Cohen et al. (2022) from passive acoustic data collected from May 2016 through April 2019 at 11 shelf break and slope monitoring sites in the western North Atlantic (Fig. 1, Table S1 in the Supplement at www.int-res.com/articles/suppl/m720p001_supp.pdf). Sites were named for co-located bathymetric or oceanographic features or adjacent anthropogenic landmarks and are referenced by their site name abbreviations (from north to south): Heezen Canyon (HZ), Oceanographer's Canyon (OC), Nantucket Canyon (NC), Babylon Canyon (BC), Wilmington Canyon (WC), Norfolk Canyon (NFC), Cape Hatteras (HAT), Gulf Stream (GS), Blake Plateau (BP), Blake Spur (BS), and Jacksonville (JAX). These sites spanned a latitudinal habitat gradient bisected by the Gulf Stream front, which follows the shelf break through the South Atlantic Bight before its separation point at Cape Hatteras, after which the current turns northeastward into the open basin. Cape Hatteras is therefore a transition point in terms of oceanographic conditions, with sites south of Cape Hatteras characterized by warm, salty, low-nutrient waters, while sites north of Cape Hatteras are characterized by cool, fresh, and productive subarctic waters.

High-frequency acoustic recording packages (Wiggins & Hildebrand 2007) with known frequency responses were deployed to continuously record sound with a sampling rate of 200 kHz, enabling analysis of signals in the 10 Hz to 100 kHz band, encompassing the frequency range of most odontocete vocalizations. Devices recorded for between 4 and 14.5 mo per deployment; serial redeployments at each site enabled minimal interruption in recording effort and balanced seasonal coverage at most sites (Table S1). Exceptions occurred at HZ, HAT, and JAX, with longer gaps of 5, 3, and 8 mo, respectively; data from these sites still captured the full seasonal cycle in 2 of the 3 study years. Only at OC were any days captured in only a single study year, when gaps between deployments happened to span the same few weeks in late May and early June in 2 consecutive years.

In total, 10 species/groups were analyzed (see Table 1), including representatives from the dolphin

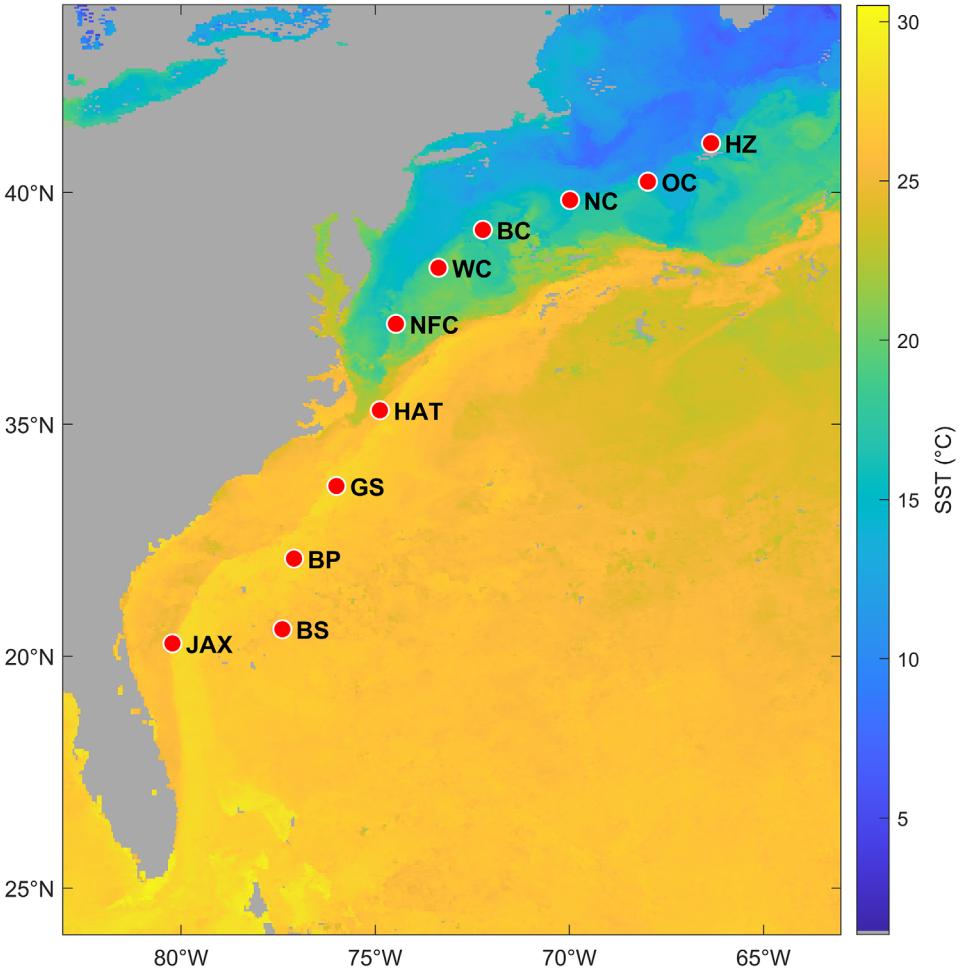

Fig. 1. Study region in the North Atlantic, with the Gulf Stream current shown by sea surface temperature (SST). Red circles: acoustic monitoring sites with site name abbreviations. HZ: Heezen Canyon; OC: Oceanographer's Canyon; NC: Nantucket Canyon; BC: Babylon Canyon; WC: Wilmington Canyon; MFC: Norfolk Canyon; HAT: Cape Hatteras; GS: Gulf Stream; BP: Blake Plateau; BS: Blake Spur; JAX: Jacksonville

and beaked whale families, sperm whales, and *Kogia* spp. Species included the short-beaked common dolphin *Delphinus delphis* (*Dd*), Risso's dolphin *Grampus griseus* (*Gg*), short-finned pilot whale *Globicephala macrorhynchus* (*Gm*), Blainville's beaked whale *Mesoplodon densirostris* (*Md*), Gervais' beaked whale *M. europaeus* (*Me*), Cuvier's beaked whale *Ziphius cavirostris* (*Zc*), Sowerby's beaked whale *M. bidens* (*Mb*), True's beaked whale *M. mirus* (*Mm*), *Kogia* spp. analyzed as a group (*Kg*), and sperm whale *Physeter macrocephalus* (*Pm*). *Gg* were identified by 2 different click types, denoted here as '*Gg1*' (canonical click type described by Soldevilla et al. 2008) and '*Gg2*' (novel click type UD36 attributed to *Gg* by Cohen et al. 2022). We analyzed these 2 *Gg* cues independently to characterize similarities or differences in their temporal occurrence. *Kogia* spp. were left as a genus-level group due to the analysis frequency band upper limit of 100 kHz, which did not fully capture the energy distribution of narrow-band, high-frequency clicks produced by both *Kogia* species and therefore did not allow for species-level discrimination.

Clicks were detected in each deployment using an automated impulse detector, clustered to identify dominant impulse types, and then a fully connected deep neural network was trained to classify detections as one of the dominant types (Frasier 2021). Many of the dominant types were attributable to known species based on previous work or were anthropogenic noise sources, but several represented novel delphinid click types, 3 of which were attributed to species through correlation with sighting data (see Cohen et al. 2022 for further details). For each species/group, we binned the time series of labeled clicks into 5 min time bins, then scaled the number of clicks per bin by effort as well as by the classifier error rates; partial effort bins only occurred at the very beginning or end of a deployment. Click counts were then converted to binomial presence–absence in each bin according to these thresholds: ≥50 clicks per 5 min bin was counted as 'presence' for delphinid species; ≥20 clicks per 5 min bin was counted as 'presence' for beaked whales, *Pm*, and *Kg*. These values were selected based on considera-

tion of the click-production rates and group sizes of these species and served to weed out presence bins based on very few detections. We considered the effect of varying these thresholds on the number and temporal distribution of bins retained in the analysis for each species and found these values to be a compromise between increasing confidence in the labels and conserving observations for analysis. This was an additional measure to reduce false positives on top of scaling the number of clicks per bin by classifier error rate. Cohen et al. (2022) carried out extensive manual verification of the automated labels, both to discard obviously incorrect labels and as a means of quantifying residual species-specific false positive rates for the remaining labels. As classifier error was found to be low except in situations where a given species had little to no presence, the scaling step generally reduced click counts in those bins to near-zeros or very low numbers, which were then mostly removed by the secondary thresholding step. Bins that remained after these 2 steps were predominantly those associated with higher numbers of clicks and lower classifier error, which we considered to be higher confidence indications of species presence. Various thresholds ranging from a few tens to several hundreds of clicks per 5 min have been used in previous odontocete studies, and in cases of extensive manual verification, the thresholding step is commonly omitted (Soldevilla et al. 2010a, 2011, Baumann-Pickering et al. 2014, 2015, Hildebrand et al. 2015, 2019, Simonis et al. 2017, Rice et al. 2021). The establishment of consistent thresholds for each species would aid in comparability across studies and through time, although issues such as differences in recording devices and detection algorithms provide additional sources of complexity in the already complex matter of detectability. Finally, species with very low presence at a given site (<100 presence bins) were not modeled at that site due to insufficient observations from which to infer reliable presence patterns, and as a final control on the reliability of the species presence data.

2.2. Temporal covariates

DOY, MPh, and time of day were used as continuous predictor variables to model species acoustic activity at 3 different temporal scales: seasonal, lunar monthly, and daily, respectively. DOY was included to capture seasonal periodicity in species activity, as this variable describes the progression through the calendar year. For the sake of this study, seasons were defined as spring, March–May; summer, June–August; fall, September–November; and winter, December–February. MPh data were calculated based on location and date using the 'getMoonIllumination' function in the R package 'suncalc' (Thieurmel & Elmarhraoui 2019) and were included to capture the progression through the lunar waxing–waning cycle. To investigate differences in diel activity patterns between species, we also included time of day as a temporal covariate. However, since our sites spanned both wide latitudinal and longitudinal ranges, we normalized the time of day to account for substantial differences in the local time of sunrise and sunset over the course of the yearly cycle. For example, a presence–absence bin at 16:00 h would coincide with sunset in New England in winter but mid-afternoon in New England in summer; in Florida, these differences would be less pronounced. This shifting relationship between hour of the day and day phase may obscure animal activity patterns that are oriented around the position of the sun, not the hands of a clock. To account for this, timestamps were linearly interpolated to the range [−1,1], with both extreme values indicating sunrise and 0 indicating sunset (a cyclic variable). A time bin situated exactly halfway through the daylight period, regardless of the duration of daylight on a given day, received a value of −0.5, while a time bin situated exactly halfway through the night period was given a value of 0.5. This representation of time preserved the situation of each time bin relative to sunrise–sunset, which we believe to be more appropriate for the investigation of diurnal patterns than local time. Study year was also included as a factor variable to account for differences between years, though the small sample size at this temporal scale (n = 3) undermines statistical power, and therefore we did not attempt to characterize interannual trends.

2.3. Statistical analysis

To quantify the significance of apparent patterns in seasonal, lunar, and diel activity, we modeled acoustic presence for each species as a response to DOY, MPh, and normalized time of day (NT) using the statistical computing software R v.4.1.1 (R Core Team 2021). We selected the multivariate generalized additive model (GAM) framework (Hastie & Tibshirani 1986), commonly used in cetacean habitat modeling (Redfern et al. 2006, Becker et al. 2014, Forney et al. 2015, Roberts et al. 2016, Frasier et al. 2021), to model a smooth function of acoustic presence (bi-

nomial data with a logit link) as a linear combination of smooth functions of our temporal covariates, yielding logistic models. These smooth functions of predictor variables capture the relationships between each predictor and the response, providing valuable insights into how species interact with the predictors. The GAM approach is popular for its ability to accommodate non-normally distributed response data — such as binomially distributed presence–absence data or Poisson-distributed count data — as well for as its interpretability. However, one of the fundamental assumptions underlying GAMs is independence of observations, a condition that is often violated by temporal or spatial autocorrelation in animal presence observations. Rather than reduce the temporal resolution of our analysis, and thereby perhaps our ability to discern diel cycles, we chose to use generalized estimating equations (GEEs) (Liang & Zeger 1986) to model the temporal autocorrelation structure directly from the data and use that structure to provide more reliable standard error estimates, an approach that has been successfully used in a number of cetacean modeling studies (Pirotta et al. 2011, Benjamins et al. 2017, Merkens et al. 2019). This approach was favored over a mixed model approach for 2 primary reasons: (1) each species' time series at a given site was serially autocorrelated but did not contain ecologically relevant groupings of data that would have been well-suited to being modeled as random effects, and (2) we were interested in using all observations to inform population-averaged parameter estimates, not in comparing parameter estimates between blocks of correlated data. The 'geeglm' function of the 'geepack' package in R (Halekoh et al. 2006) was used. This function uses a GEE approach to fit a linear model as opposed to the more typical iteratively reweighted least-squares approach. The 'geeglm' function requires a grouping variable indicating blocks within which data are known to be correlated, and between which independence is assumed. To determine the most appropriate block size for each species at each site, we calculated the autocorrelation function (ACF) of our presence time series using the 'acf' function in the base R package 'stats' and inspected plots of ACFs. A first-order autoregressive ('ar1') correlation structure was used for all models based upon inspection of the ACF plots.

To obtain smooth functional relationships between the temporal predictor variables and the response, we extended the GEEGLM framework to a GEEGAM. DOY, MPh, and NT were supplied to the models as cyclic splines using the 'mSpline' function in the R package 'splines2' (Wang & Yan 2021). Cyclicity was desired to coerce continuity between, e.g. 31 December and 1 January, represented by DOYs 365 and 1, respectively. To determine the optimal number of knots to use in the splines, we fit simple univariate models with a range of knot values, from 4 (minimum required for a cyclic variable in 'mSpline') to 8, and compared the quasilikelihood information criterion (QIC). The QIC is an analog of Akaike's information criterion that is suitable for GEEs, which use QIC-based methods rather than maximum likelihood-based methods (Pan 2001). We found that for all 3 smooth covariates, splines with 5 knots had the lowest QIC values for the majority of our models, indicating the most favorable tradeoff between model fit and complexity. We also noted that DOY splines with just 4 knots did not allow enough flexibility to capture the bimodality in presence that we observed in some of our histograms of presence versus DOY. Rather, such inflexible splines would overly smooth the 2 peaks, resulting in an estimated single peak in presence right at the time of an actual trough in presence. Therefore, we chose to use 5 knots for all 3 smooth terms in all models, both for consistency and to allow sufficient flexibility.

An interaction term was included between DOY and NT to account for the possibility of changes in diel patterns over the course of the seasonal cycle. We believed this interaction to have ecological relevance given the seasonal variation in prey availability throughout the year and the likely necessity for plasticity in foraging behavior. An interaction term between NT and MPh was also included. Lunar cycles have been shown to be significant for some odontocete species (Simonis et al. 2017, Owen et al. 2019), although it is uncertain whether these patterns are driven by the magnitude of lunar illumination and its impact on the depth distribution of diel vertically migrating prey (Kampa 1975, Last et al. 2016) or if the patterns are the result of endogenous circadian rhythms. If lunar cycles are driven by lunar illuminance, then we would expect to see the most pronounced impact on cetacean activity at night, as lunar illuminance during the day is negligible compared to solar illuminance. By including this interaction, we were able to consider lunar cycles exhibited during the dark hours independent of any patterns present during the daytime.

The deployment location at HAT shifted northeastward along the slope by about 33 km after the first study year (northern site shown in Fig. 1). This shift moved our device away from the direct flow of the Gulf Stream, resulting in obvious changes in species

presence between the first study year and the second 2 years. Therefore, we judged that the deployments spanning this move could not be considered contiguous or representative of the same habitat. Data from the first study year at HAT were not used; models were only constructed at HAT for those species that exhibited sufficient presence in the second and third study years. *Kogia* spp. (the dwarf and pygmy sperm whales) were also not modeled at any of the northern sites because the sampling frequency of 200 kHz limited the acoustic analysis of Cohen et al. (2022) to a Nyquist frequency of 100 kHz, making *Kogia* spp. identifiable only by click spectra with highest amplitudes above 90 kHz, resulting from aliased energy (Hildebrand et al. 2019). Since the full click spectra could not be resolved, we had no way of differentiating apparent *Kogia* spp. clicks from similarly narrowbandwidth, high-frequency harbor porpoise *Phocoena phocoena* clicks in the northern region, where these species co-occur along the shelf break (Gaskin 1984).

Full models with all 4 temporal predictors plus 2 interactions were initially run for all species at all sites meeting a minimum presence criterion of ≥100 presence bins across the entire study period (see Table 1), barring the exceptions mentioned above. For each model, the marginal significance of each term was calculated by fitting repeated ANOVAs with each model term in the last position; non-significant terms were removed and models were re-run in a stepwise fashion until only significant terms remained in each model (see Table 3). If one or both terms contributing to an interaction were not significant on their own but the interaction was significant, then both contributing terms were retained.

To assess model fit, we examined binned residual plots and computed McFadden's pseudo-R^2, which are better suited to evaluating logistic models than traditional residuals-versus-fitted value plots and R^2 due to these models' non-normal response and discrete residuals (see Table 2). Binned residual plots provide insights about model over/under prediction by quantifying the proportion of binned residuals that fall outside the 95% confidence intervals (Gelman & Hill 2006). Systematic over/under prediction may indicate that the model does not account for all of the variability in the observations. McFadden's pseudo-R^2 (ρ^2) compares the log likelihood of a fitted model to the log likelihood of the null model, with values ranging from 0, indicating no improvement upon the null model, to 1, indicating the saturated model (perfectly overfit, not desirable) (McFadden 1973). McFadden's pseudo-R^2 is numerically equivalent to deviance explained for logistic regression models since the log likelihood of the null logistic model is always 0. As very high values of ρ^2 indicate overfitting, this metric should be judged somewhat differently than values of traditional R^2. McFadden remarked that ρ^2 in the range of 0.2–0.4 should be considered indicative of excellent fit (McFadden 1977). McFadden's pseudo-R^2 was favored over another pseudo-R^2 for logistic regression — Tjur's coefficient of discrimination — because the latter is not well-suited to cases of low presence and low overall predicted probability of presence, which was the case for most of our models.

Inspection of the binned residual plots showed that model performance was highly variable, with the quality of fit tightly correlated with the level of presence the model was fitted to; models based on fewer than ~1000 presence bins generally performed poorly. Therefore, we chose to set a minimum threshold of ≥60% of binned residuals within the 95% confidence intervals and do not report here on models that did not meet this criterion to avoid drawing spurious conclusions from ill-fitting models. We arrived at this conservative threshold based on consideration of the limits of these models — many influential factors were beyond the scope of this study, and temporal covariates are not expected to account for all the variability in animal presence or activity. In recognition of the challenges of modeling noisy and imperfectly sampled ecological phenomena, ecological models are typically considered to have good explanatory power when R^2 exceeds 0.25 (Cohen 1988, Møller & Jennions 2002). The binned residuals method should not be interpreted as analogous to R^2, but similar considerations about the explanatory power of these models guided our choice of threshold. About two-thirds of our models (57 of 83) satisfied this criterion and are discussed here, while the remaining one-third (26) were considered too unreliable to interpret (see Table 2).

Partial residual plots of the smooth functions of significant terms were also compared to histograms of presence binned across observed values of our covariates to verify that the patterns estimated by the models were reflective of the underlying data. Details of the method for visualizing interactions of smooth terms are given in Text S1. Coefficients of overlap (Δ) were computed for species with similar diving ecology that co-occupied a given site, using the 'overlap' package in R (Ridout & Linkie 2009) to quantify temporal co-occurrence. We first used the 'densityPlot' function to fit a kernel density function to each species' presence at a given site and then used the 'overlapTrue' function to quantify overlap between the

normalized kernel density functions of 2 species. Δ values obtained using this approach can range between 0, indicating absolutely no simultaneous presence, to 1, indicating perfect co-occurrence.

3. RESULTS

Acoustic recording effort was continuous at each site except for brief gaps between deployments and a few larger gaps at selected sites, as noted earlier (Table S1). Species presence varied across sites by 3 orders of magnitude (Table 1). Distinct patterns of spatial and seasonal distribution were observed as detailed below and illustrated by partial residual plots of the smooth functions of each temporal predictor. The *y*-scales of partial residual plots are presented here in units of the transformed response variable (logits), as determined by the link function. We were interested more in the shapes of the functional relationships estimated by the models than the precise values predicted for probability of presence, and as the predicted probability of presence based on any one predictor variable depends on several factors (e.g. what other variables were included in the model, what their explanatory power was, the level of presence observed for a given species at a given site), we did not consider it productive to back-transform these units to derive predicted probability of presence.

Models that exceeded the binned residuals threshold were generally well-fit according to the binned residuals metric (Table 2), with more than half (29 of 57) exceeding 80% and an additional 17 models falling between 73 and 80%. Eleven models fell into the range of 60–70%: *Mb* at OC; *Mm* at NC and NFC (the only models retained for this species); *Pm* at WC, NFC, and HAT; Risso's *Gg1* click type at JAX and *Gg2* click type at HZ and OC; and *Gm* at OC and GS. Data paucity was not always responsible for lower performance, as these models were fit to between 555 and 35 889 presence bins. McFadden's pseudo-R^2 values for the retained models ranged from 0.008 to 0.276; slightly less than half (24 of 57) had values of >0.1 (Table 2). These values indicate that most of our models only account for a modest amount of variability in the response, although a few meet the criterion for 'excellent' fit ($\rho^2 > 0.2$) proposed by McFadden (e.g. *Dd* at BC, WC, and NFC).

3.1. Regional differentiation

The acoustic presence of all species exhibited clear preferences either for or against Gulf Stream waters (Fig. 2). Most species had higher levels of presence in the north; only *Md*, *Me*, and *Kg* primarily occupied the southern stations, which are characterized by the strong influence of the Gulf Stream.

Within the northern and southern regions, the beaked whales also exhibited distinctly different patterns of primary site occupancy. In the south, *Me* were present at GS, BP, and BS, with a marked peak at GS, while *Md* were present almost exclusively at BS. In the north, *Zc*, *Mb*, and *Mm* occupied many of the same sites, but their sites of primary occupancy were non-overlapping. *Zc* were most abundant at

Table 1. Acoustic recording sites, effort, and species presence. Effort across the 3 yr study period is given as cumulative days of acoustic data at each monitoring site; presence of each species is given as a percent of effort with presence. Zero values indicate presence of <0.05%; grey shading indicates where low presence either obviated or challenged modeling efforts (see Table 2 for model fit metrics). *Dd*: short-beaked common dolphin; *Gg1* and *Gg2*: Risso's dolphin click types; *Gm*: short-finned pilot whale; *Md*: Blainville's beaked whale; *Me*: Gervais' beaked whale; *Zc*: Cuvier's beaked whale; *Mb*: Sowerby's beaked whale; *Mm*: True's beaked whale; *Kg*: *Kogia* spp.; *Pm*: sperm whale

Site	Lat., Long.	Depth (m)	Effort (d)	Percent species presence										
				Dd	*Gg1*	*Gg2*	*Gm*	*Md*	*Me*	*Zc*	*Mb*	*Mm*	*Kg*	*Pm*
Heezen Canyon (HZ)	41.06° N, 66.35° W	890	926	16.7	3.9	0.7	1.4	0	0	1.7	1	0.1	0	14.3
Oceanographer's Canyon (OC)	40.23° N, 67.98° W	450/880	990	16	5	0.5	0.4	0	0	0.2	0.2	0.2	0	13.2
Nantucket Canyon (NC)	39.83° N, 69.98° W	900	1041	16.4	8.2	2.3	0.6	0	0	0.1	0.1	0.4	0	18.9
Babylon Canyon (BC)	39.19° N, 72.23° W	1000	1075	20.6	6	2.5	1.5	0	0	0.4	0.4	0.2	0.1	12
Wilmington Canyon (WC)	38.37° N, 73.37° W	1040	1094	24.7	4.3	1.4	3.1	0	0	1.5	1.1	0.2	0	9
Norfolk Canyon (NFC)	37.16° N, 74.47° W	1110	1093	26	1.4	0.9	6.7	0	0	0.3	0.2	0.3	0	9.9
Hatteras (HAT)	35.30° N, 74.88° W	1210	1001	21	0.4	0.1	8	0	1	13.3	0.1	0	0	12.4
Gulf Stream (GS)	33.67° N, 76.00° W	930	1092	1.3	0.4	0.1	0.8	0	7.8	0	0	0	0.3	3
Blake Plateau (BP)	32.11° N, 77.09° W	950	1094	2.1	0.1	0	0.1	0	4.6	0	0	0	0.2	0.5
Blake Spur (BS)	30.58° N, 77.39° W	1050	1090	2.4	0.1	0	0.1	2.8	0.8	0.1	0	0	0.4	1.7
Jacksonville (JAX)	30.28° N, 80.22° W	750	853	4	1.8	0.1	0.9	0	0	0	0	0	0.2	1.1

Table 2. Model fit given by percent of binned residuals and McFadden's pseudo-R^2. %BR: percent of binned residuals that fell within the 95% CIs. In a perfectly fitted model, about 95% of the residuals would be expected to fall within these bounds. McFadden's pseudo-R^2 (ρ^2) compares the log likelihood of a fitted model to the log likelihood of the null model. Small values indicate performance similar to the null model, while a value of 1 would indicate perfect model fit (i.e. fully saturated model, completely overfit). McFadden commented that these values are typically much smaller than traditional R^2 values and that ρ^2 in the range of 0.2–0.4 represents 'an excellent model fit'. Blank cells: modeling was not undertaken due to low presence; grey shading: model fit did not meet the criterion of ≥60% binned residuals within the 95% CIs; patterns from these models are not presented. Site and species abbreviations as in Fig. 1, Table 1

	Dd		*Gg1*		*Gg2*		*Gm*	
	%BR	ρ^2	%BR	ρ^2	%BR	$<\rho^2$	%BR	ρ^2
HZ	0.736	0.132	0.767	0.173	0.647	0.117	0.880	0.061
OC	0.826	0.114	0.740	0.168	0.629	0.093	0.605	0.087
NC	0.834	0.152	0.832	0.070	0.860	0.163	0.763	0.059
BC	0.851	0.223	0.804	0.071	0.812	0.213	0.781	0.149
WC	0.804	0.223	0.785	0.130	0.767	0.162	0.822	0.136
NFC	0.729	0.276	0.822	0.046	0.740	0.117	0.849	0.111
HAT	0.847	0.131	0.476	0.075			0.860	0.109
GS	0.859	0.060	0.403	0.144	0.175	0.110	0.669	0.122
BP	0.822	0.102	0.332	0.106			0.383	0.073
BS	0.789	0.124	0.280	0.083			0.363	0.081
JAX	0.798	0.107	0.669	0.146	0.270	0.142	0.581	0.227

	Md		*Me*		*Zc*		*Mb*	
	%BR	ρ^2	%BR	ρ^2	%BR	$<\rho^2$	%BR	ρ^2
HZ					0.824	0.074	0.890	0.015
OC					0.418	0.078	0.603	0.022
NC					0.265	0.063	0.370	0.046
BC					0.840	0.009	0.759	0.014
WC					0.865	0.020	0.899	0.013
NFC					0.581	0.046	0.574	0.019
HAT					0.862	0.022		
GS	0.141	0.107	0.777	0.031	0.164	0.057		
BP	0.128	0.045	0.843	0.037				
BS	0.818	0.019	0.841	0.016	0.313	0.024		
JAX								

	Mm		*Kg*		*Pm*	
	%BR	ρ^2	%BR	ρ^2	%BR	ρ^2
HZ	0.386	0.049			0.787	0.036
OC	0.309	0.138			0.805	0.059
NC	0.613	0.071			0.860	0.037
BC	0.361	0.011			0.749	0.045
WC	0.518	0.035			0.674	0.073
NFC	0.649	0.042			0.640	0.145
HAT					0.634	0.162
GS			0.574	0.066	0.847	0.016
BP			0.587	0.032	0.859	0.009
BS			0.796	0.008	0.793	0.050
JAX			0.500	0.029	0.226	0.064

HAT, with presence one or 2 orders of magnitude lower in the north. *Mb* exhibited 2 preferred loci of presence: one at HZ and another at WC. Detections of *Mm* were strongest at NC, where both *Zc* and *Mb* were conspicuously absent despite occupying neighboring sites.

Distribution patterns of the 3 dolphin species were dissimilar from one another. *Dd* exhibited high levels of presence across the study area, albeit with a bias towards the northern region. *Gg* exhibited a stronger preference for northern sites, shown by negligible presence of both click types in the south, except at JAX. *Gm* had their strongest occurrence at HAT and NFC, with lower presence at the more northerly sites and JAX, and negligible occupation of BP and BS. *Pm* exhibited a regional distribution similar to *Dd*, with presence at all sites but a bias towards the northern sites. *Kg* exhibited low levels of presence at all sites south of HAT.

3.2. Seasonal fluctuations in presence across species

The seasonal cycle, represented by DOY, was highly significant ($p < 0.001$) in almost all retained models (Table 3). Most DOY patterns were unimodal, with a peak in presence during one season; the season of peak presence varied across species (Fig. 2). However, in some cases, bimodal patterns with 2 distinct seasonal peaks in presence occurred (see e.g. Fig. 3); we considered patterns to be meaningfully bimodal when the 95% confidence intervals of a trough in predicted presence fell below the 95% confidence intervals of the peaks on either side.

The DOY patterns for *Dd* were consistent across most sites, with presence peaking in the spring between BS in the south and NC in the north; peaks fell later in the summer at OC and HZ (the northernmost sites) and at JAX (the southernmost site) (Fig. 3). This was similar to the seasonal patterns of *Gg* at the sites where both species occurred. *Dd* did not appear to meaningfully occupy any of the sites during the fall.

The 2 *Gg* click types present in the data set showed seasonal patterns similar to one another north of HAT

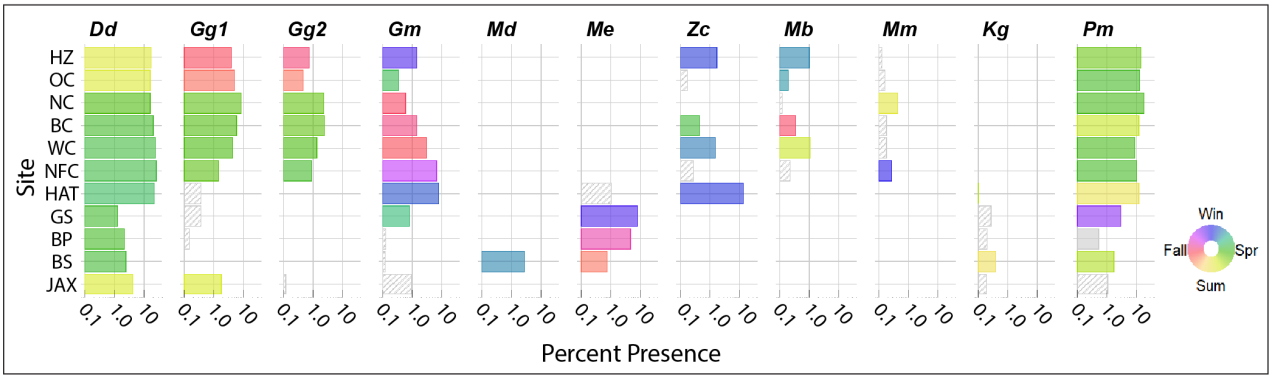

Fig. 2. Site occupancy and seasonal peak presence by species and site. Bar length gives presence bins per thousand effort bins; note the *x*-axis is in log scale. Color shows the day-of-year value of peak presence in models for which day-of-year was significant; gray fill indicates that day-of-year was not significant. Stripes indicate no model due to insufficient presence or poor model performance. Site and species abbreviations as in Fig. 1, Table 1

(Fig. 3): in spring they were found in the mid-Atlantic Bight, whereas in fall they were more present at the northernmost sites, such as HZ. The boundary for this seasonal shift occurred at NC, where the *Gg1* click type exhibited a spring–fall bimodality that was indistinct or absent for *Gg2*. Similar spring–fall bimodality was seen for *Gg1* at NFC but not for *Gg2*. Despite lower model performance for *Gg2* at HZ and OC (Table 2), the seasonal patterns estimated are consistent with those suggested by histograms of the presence binned with monthly resolution. Presence of both *Gg* click types was quite low from HAT southward and was not possible to model, except for *Gg1* at the JAX site, where model performance was not as good as at the northern sites (Table 2). *Gg* were absent from all sites in the winter.

Gm were most abundant at HAT, where they exhibited peak presence in the winter (Fig. 2). At the northern sites, *Gm* exhibited peak presence in early winter and fall from NFC to BC, and bimodal spring–fall peaks at NC giving way to a winter peak at HZ; except for shared bimodality with *Gg* at NC, this pattern was dissimilar from the seasonal presence of the other delphinid species at the same sites (Fig. 3). An apparent incongruity at these northern sites, the spring peak in *Gm* presence at OC was actually the continuation of elevated presence beginning in the fall and continuing through winter and into the spring; relatively poor model performance (Table 2) and wider confidence intervals for this estimated seasonal pattern show that spring and fall peaks may not be truly different and that these predictors leave much variability in species presence unaccounted for. We observed that *Gg* and *Gm* had staggered seasonal peaks at sites where their ranges overlap and did not generally occupy a given site at the same time. Coefficients of overlap for *Gg* and *Gm* at the northern sites were generally low, ranging from 0.32 to 0.54, except at site NC, where overlap was more substantial at $\Delta = 0.73$ (Table 4).

A clear temporal separation was apparent for the southern beaked whale species at BS, where *Md* presence peaked in the late winter, while *Me* presence peaked in the fall (Fig. 4); however, the coefficient of overlap ($\Delta = 0.70$) suggests substantial co-occurrence despite these differing seasonal peaks (Table 4). In the north, *Zc* and *Mb* both occupied the sites from NFC to HZ (Fig. 2, Table 1), but available seasonal patterns suggested that they were temporally separated at these sites (Fig. 4). At BC and WC, *Mb* presence peaked in the fall and summer, respectively, while *Zc* peaked in the spring and late winter, respectively. At HZ, *Mb* and *Zc* presence peaked in early spring and winter, respectively, which suggests some co-occurrence at this site. The apparent temporal separation suggested by these seasonal peaks was not well-supported by the coefficient of overlap values at these sites, which ranged from 0.74 to 0.81 (Table 4), indicating substantial temporal co-occurrence despite differing seasons of peak presence. At NC, their site of primary occupancy, *Mm* exhibited slightly bimodal summer and winter peaks in presence. While both the *Mm* models were on the lower end of model performance, the seasonal patterns they estimated matched well with those suggested by histograms of the presence binned with monthly resolution. Most beaked whale species exhibited a winter peak in presence at their sites of highest occupancy, regardless of whether those sites were in the south or north (Figs. 2 & 4).

Peak presence of *Pm* occurred during the spring and summer at most sites (Fig. 4). Model performance

was somewhat lower at HAT, NFC, and WC (Table 2), although presence was high. Despite this lower performance, the seasonal patterns estimated at those sites are aligned with the seasonal peaks seen in histograms of presence binned with monthly resolution. At HZ and OC, bimodality was apparent, with a higher peak in the spring and a lower peak in the fall. GS was the only site where *Pm* presence peaked in the winter. While the DOY smooth for *Kg* at BS suggested a summer peak in presence, the confidence intervals were wide. Examination of the raw data showed that the summer peak in presence was inconsistent: it was particularly pronounced during July of the first study year, was lower amplitude and shifted earlier to June in the second study year, and no clear summer peak was discernible in the third study year. The strong pattern in

Table 3. Term significance for each model by species and site. Yr: study year; DOY: day-of-year; MPh: moon phase; NT: normalized time of day. ***p < 0.001; **p < 0.01; *p < 0.05; NS: not significant. (–) denotes models with poor fit, which are not presented here; blank cells indicate modeling was not undertaken due to low presence. Site and species abbreviations as in Fig. 1, Table 1

	Dd						*Md*					
	Yr	DOY	MPh	NT	NT: DOY	NT:MPh	Yr	DOY	MPh	NT	NT: DOY	NT:MPh
HZ	***	***	**	***	***	*						
OC	***	***	***	***	***	***						
NC	***	***	***	***	***	***						
BC	***	***	***	***	***	**						
WC	***	***	***	***	***	***						
NFC	***	***	**	NS	***	***						
HAT	***	***	***	***	***	***						
GS	***	***	*	NS	*	NS	–	–	–	–	–	–
BP	***	***	***	***	***	NS	–	–	–	–	–	–
BS	***	***	**	***	***	***	***	***	***	***	**	NS
JAX	***	***	NS	***	***	***						
	Gg1						*Me*					
	Yr	DOY	MPh	NT	NT: DOY	NT:MPh	Yr	DOY	MPh	NT	NT: DOY	NT:MPh
HZ	***	***	***	***	***	NS						
OC	***	***	NS	***	***	NS						
NC	***	***	***	***	***	***						
BC	***	***	***	NS	***	**						
WC	***	***	***	***	***	***						
NFC	***	***	NS	***	***	***						
HAT	–	–	–	–	–	–						
GS	–	–	–	–	–	–	***	***	***	***	NS	*
BP	–	–	–	–	–	–	***	***	***	***	***	NS
BS	–	–	–	–	–	–	**	***	**	***	**	NS
JAX	***	***	NS	***	**	***						
	Gg2						*Zc*					
	Yr	DOY	MPh	NT	NT: DOY	NT:MPh	Yr	DOY	MPh	NT	NT: DOY	NT:MPh
HZ	***	***	NS	***	***	**	*	***	***	***	**	NS
OC	***	***	*	***	***	***	–	–	–	–	–	–
NC	***	***	***	***	***	NS	–	–	–	–	–	–
BC	***	***	NS	***	***	*	NS	***	NS	***	NS	*
WC	***	***	***	***	***	**	NS	***	***	***	**	NS
NFC	***	***	NS	***	***	***	–	–	–	–	–	–
HAT							***	***	**	***	***	***
GS	–	–	–	–	–	–	–	–	–	–	–	–
BP												
BS							–	–	–	–	–	–
JAX	–	–	–	–	–	–						

(*continued on next page*)

Table 3 (continued)

	Gm						*Mb*					
	Yr	DOY	MPh	NT	NT: DOY	NT:MPh	Yr	DOY	MPh	NT	NT: DOY	NT:MPh
HZ	***	***	NS	***	***	***	***	***	***	***	NS	*
OC	***	***	***	***	***	***	***	***	NS	***	***	*
NC	***	***	**	***	***	***	–	–	–	–	–	–
BC	***	***	*	***	***	***	***	***	NS	***	***	NS
WC	***	***	***	***	***	***	***	***	***	***	NS	NS
NFC	***	***	NS	***	***	***	–	–	–	–	–	–
HAT	***	***	***	***	***	***						
GS	***	***	***	***	***	***						
BP	–	–	–	–	–	–						
BS	–	–	–	–	–	–						
JAX	–	–	–	–	–	–						

	Mm						*Pm*					
	Yr	DOY	MPh	NT	NT: DOY	NT:MPh	Yr	DOY	MPh	NT	NT: DOY	NT:MPh
HZ	–	–	–	–	–	–	***	***	***	***	***	NS
OC	–	–	–	–	–	–	***	***	***	***	***	*
NC	***	***	NS	***	**	NS	***	***	NS	***	***	*
BC	–	–	–	–	–	–	***	***	X	***	***	X
WC	–	–	–	–	–	–	***	***	**	***	**	NS
NFC	***	***	NS	***	NS	NS	***	***	***	***	***	*
HAT							***	***	NS	NS	***	**
GS							NS	***	NS	NS	*	NS
BP							NS	NS	NS	NS	**	NS
BS							NS	***	***	***	**	*
JAX							–	–	–	–	–	–

	Kg					
	Yr	DOY	MPh	NT	NT: DOY	NT:MPh
HZ						
OC						
NC						
BC						
WC						
NFC						
HAT						
GS	–	–	–	–	–	–
BP	–	–	–	–	–	–
BS	*	*	***	***	NS	NS
JAX	–	–	–	–	–	–

the first year may be driving the significant p-value for DOY in this model, while the interannual variability likely underlies the parameter estimate variability.

3.3. Lunar cycles were most impactful for delphinids

MPh was significant in most of the models, and often interacted significantly with NT; most of the instances of non-significance were in models for deep divers (Table 3). The interaction between MPh and NT was included to enable consideration of the lunar patterns exhibited at night, when we would expect the influence of lunar illumination to be most pertinent. Despite being a significant interaction in many cases, the lunar patterns did not always appear to be different between daytime and nighttime. This may indicate that the interaction was one way (MPh influenced diel pattern, but diel phase did not influence lunar pattern).

The most coherent lunar patterns were seen for the dolphin species (Fig. 5). *Dd* exhibited a preference

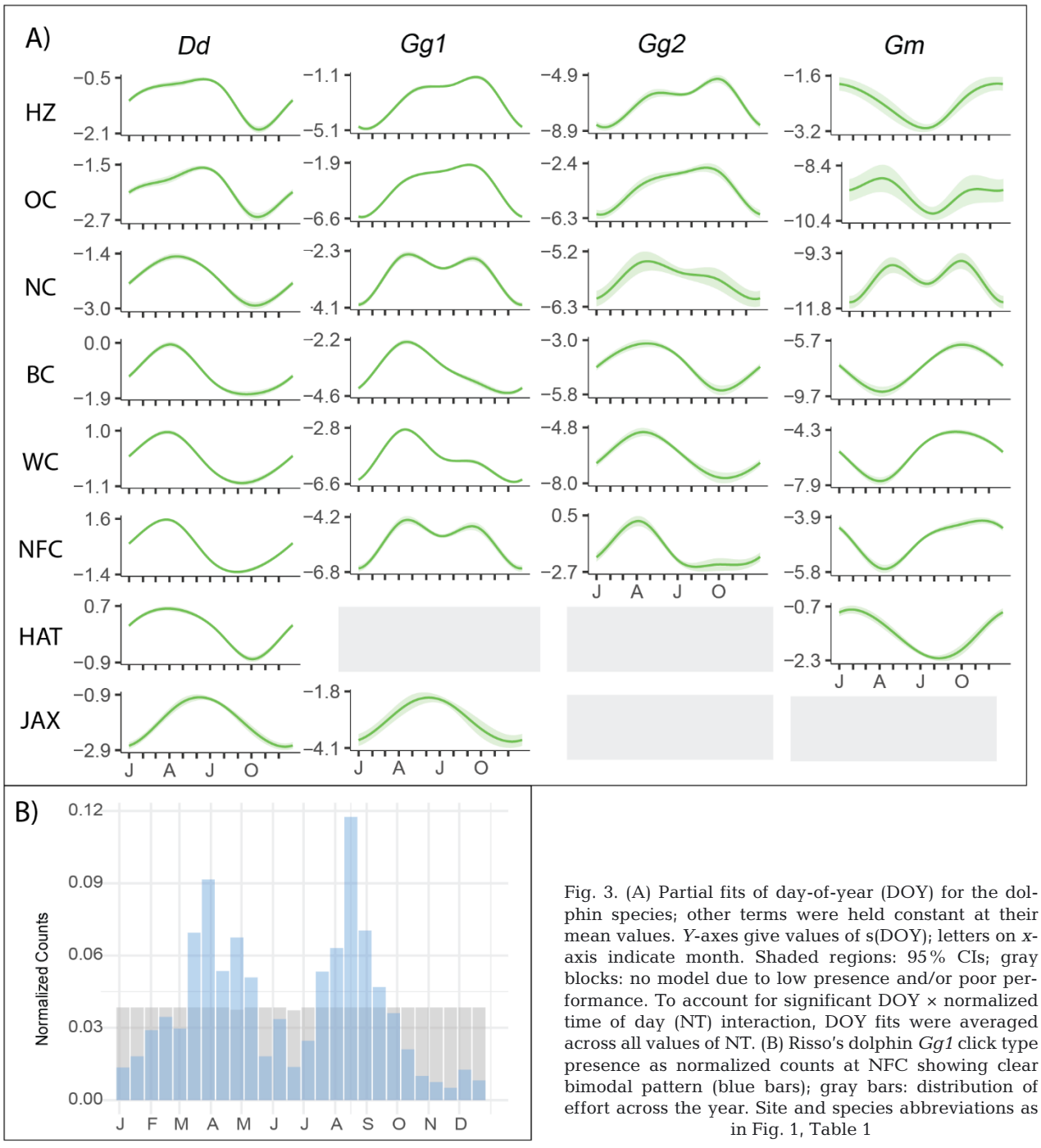

Fig. 3. (A) Partial fits of day-of-year (DOY) for the dolphin species; other terms were held constant at their mean values. *Y*-axes give values of s(DOY); letters on *x*-axis indicate month. Shaded regions: 95% CIs; gray blocks: no model due to low presence and/or poor performance. To account for significant DOY × normalized time of day (NT) interaction, DOY fits were averaged across all values of NT. (B) Risso's dolphin *Gg1* click type presence as normalized counts at NFC showing clear bimodal pattern (blue bars); gray bars: distribution of effort across the year. Site and species abbreviations as in Fig. 1, Table 1

for the new moon at night at most of the sites; daytime lunar preferences were more variable, consistent with our expectation that the lunar influence would be most impactful at night if lunar illuminance was the driving consideration. *Gm*, on the other hand, exhibited a consistent preference for the full moon at night and generally against the full moon during the day. Neither of the *Gg* click types exhibited lunar patterns that were consistent across sites or in keeping with the light preferences suggested by their diel cycles (discussed below).

A lower proportion of the beaked whale models indicated an interaction between MPh and NT than was seen for the dolphin models (45% compared to 87%), and in 4 of 5 such models, the confidence intervals were wide and overlapping, indicating that parameter estimates contained high variability (Fig. S1). Differences between the daytime and

Table 4. Coefficient of overlap (Δ) for species with similar foraging ecology that occupy the same sites. Values can range from 0 to 1, with small values indicating little or no co-occurrence and values approaching 1 indicating almost perfect co-occurrence

Species	Site	Δ
Risso's dolphin and short-finned pilot whale	HZ	0.4126
	OC	0.5050
	NC	0.7336
	BC	0.4148
	WC	0.3193
	NFC	0.5439
Cuvier's and Sowerby's beaked whales	HZ	0.7425
	BC	0.8070
	WC	0.7951
Blainville's and Gervais' beaked whales	BS	0.6977

nighttime lunar patterns in these cases may not be reliable or ecologically meaningful. *Pm* exhibited variable lunar patterns across the sites for which the term was significant but a preference for the full moon at night could be seen (Fig. S1). The pattern for *Kg* had wide confidence intervals, similar to the DOY and NT patterns for this group (Fig. S1).

3.4. Diel patterns change across the seasonal and lunar cycles

NT was significant in all retained models and usually interacted significantly with DOY and/or MPh (Table 3). The interaction between NT and DOY revealed substantial changes in diel patterns throughout the year for some species. Differences in the magnitude of the smooth functions of NT across seasons may be a function of seasonally varying probability of presence and/or the relative importance of the diel cycle throughout the year. Diel patterns did not vary as much across the lunar cycle, suggesting the lunar influence is less important in driving odontocete diel activity patterns than the seasonal influence. However, when there was modulation of the diel pattern across the lunar cycle, variability in activity was almost exclusively confined to the nighttime hours. This supports the hypothesis that the impact of the lunar cycle on odontocetes is a function of lunar illumination, which is only relevant at night. We focus here primarily on diel patterns exhibited by each species during their periods of peak presence at a given site. Fig. 6 provides a summary of the partitioning of presence between diel phases for each species at each site during the 90 d period centered on their seasonal peak in presence; this partitioning was calculated based on the raw presence data, not model output. A selection of illustrative partial smooth plots from the temporal models, showing diel patterns at different points in the seasonal and lunar cycles, is shown below; the remaining partial smooth plots can be seen in the Supplement (Figs. S2–S8).

Dd diel patterns showed a preference for dark conditions across sites and seasons, with the highest levels of acoustic activity at night; occasionally a slight preference for dusk or dawn was visible (e.g. Fig. 7A). Differences in diel patterns at different points in the lunar cycle were mostly trivial (e.g. Fig. 7A), although we did observe that at sites where the NT and MPh interaction was significant, the highest levels of nighttime activity were generally during new and/or waxing moons. These differences were more pronounced at HAT and JAX; nighttime activity at HAT was suppressed during the full moon in all seasons (Fig. 7B).

During their seasons of peak presence, *Gg* exhibited varying diel patterns across sites; within sites, diel patterns changed across the seasonal cycle (e.g. Fig. 8A). Considering only diel patterns exhibited during seasons of peak presence, *Gg1* showed a nocturnal pattern at the northernmost sites HZ and OC in the fall; a crepuscular pattern at the mid-Atlantic Bight sites NC, BC (Fig. 8A), and, less so, WC, in the spring; and a nocturnal pattern in the south at JAX in the summer. Despite lower model performance at JAX, this nocturnal preference matches the strong nocturnal pattern shown by histograms of presence binned with hourly resolution. *Gg2* had distinctly different diel patterns during the same seasons at the same sites: crepuscular with some nocturnal activity at the northernmost sites HZ and OC in the fall and diurnal at NC, BC (Fig. 8B), and WC in the spring. The *Gg2* models had poorer performance at HZ and OC and parameter estimates for diel patterns had wide confidence intervals, so these diel patterns may not be strong or consistent. Both the *Gg* click types exhibited some variability in diel pattern that was modulated by the lunar cycle, although at most sites the overall shape of the diel pattern was conserved across the lunar cycle. A notable exception occurred during the *Gg2* spring presence peak at NFC, when the pattern was most strongly diurnal during the waning moon, with little diel preference indicated by wide and overlapping confidence intervals predicted at other points in the lunar cycle (Fig. 8C).

Gm exhibited a preference for well-illuminated conditions with generally diurnal echolocation be-

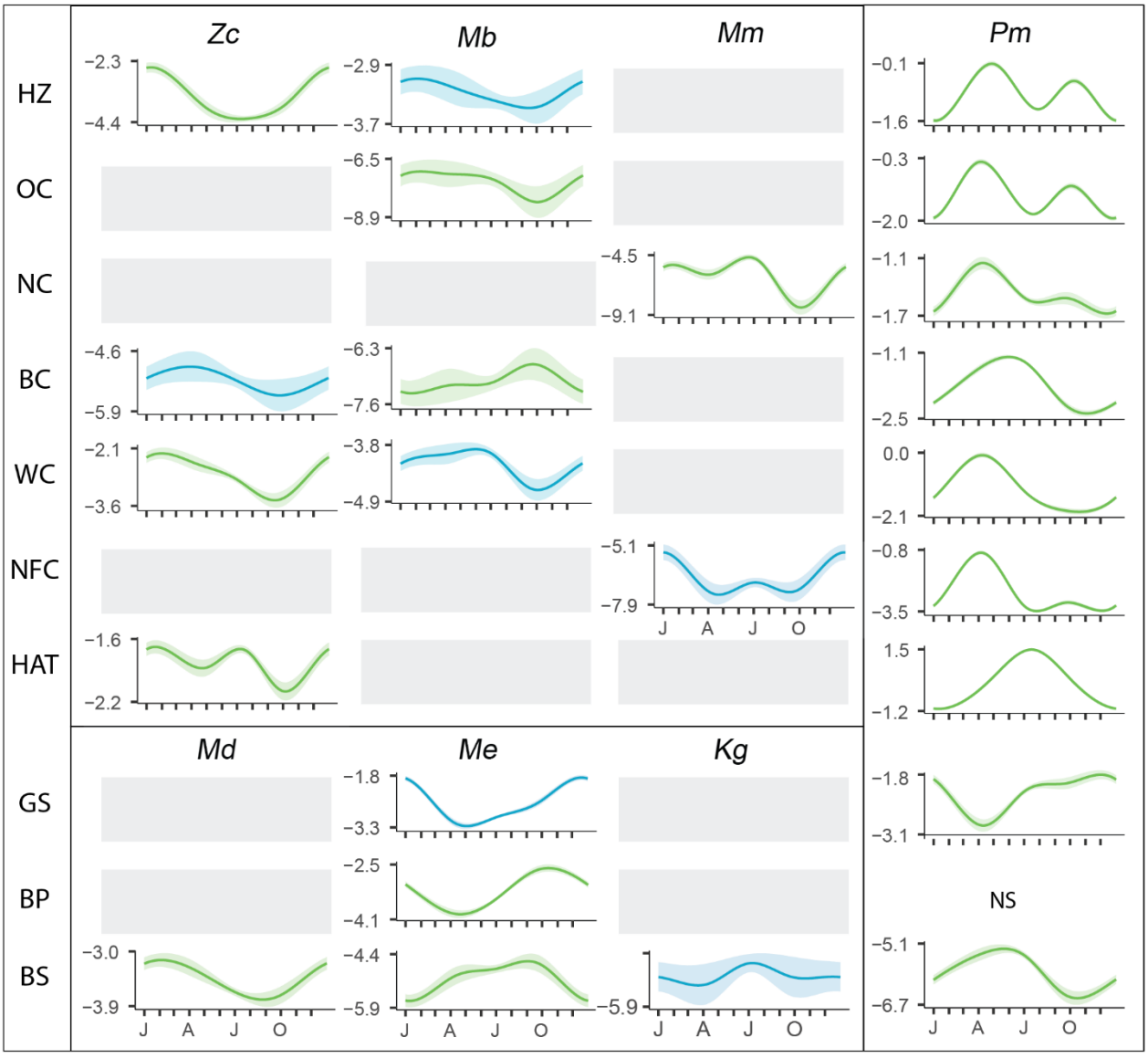

Fig. 4. Partial fits of day-of-year (DOY) for the beaked whales, *Kogia* spp., and sperm whales; other terms were held constant at their mean values. *Y*-axes give values of s(DOY); letters on *x*-axis indicate month. Shaded regions: 95% CIs; gray blocks: no model due to low presence and/or poor performance; NS: DOY was not significant. Blue lines: no significant interaction between DOY and normalized time of day (NT); green lines: significant DOY × NT interaction, for which DOY fits were averaged across all values of NT. Site and species abbreviations as in Fig. 1, Table 1

havior across seasons at HAT and NFC, their sites of peak presence (Fig. 6). At the northern sites, pilot whales exhibited crepuscular behavior during their seasons of peak presence, often with a dawn preference. The model at OC had poorer performance, and parameter estimates for diel patterns had wide confidence intervals, so diel patterns at that site may not be strong or consistent. Nighttime activity levels from HAT to NC were highest during periods of lunar illumination, e.g. at HAT in the spring nighttime activity during the full moon rivaled daytime activity (Fig. 9) At OC and HZ, this pattern changed, with highest levels of nighttime activity around the waning and waxing moons in all seasons.

Diel patterns for the beaked whales often had wide and overlapping confidence intervals when looking across points in the lunar and seasonal cycles, perhaps arising from inconsistent patterns across the study period (Figs. S6 & S7). The diel pattern for *Kg* suggested an anti-dusk preference, but as with the other smooth terms for this species, confidence intervals were wide and the true pattern may not be different from a flat line (Fig. S7). *Pm* were the only deep divers to exhibit convinc-

ing diel patterns (clear differences between daytime and nighttime activity, narrow confidence intervals) across sites, but these patterns were highly variable between sites and seasons and included diurnal, nocturnal, dawn preference, dusk avoidance, and dawn avoidance patterns (Fig. S8). At HAT and BS, *Pm* nighttime activity was always highest around the full moon.

4. DISCUSSION

The long-duration, continuously sampled data used here allowed us to analyze toothed whale presence at a range of temporal scales — yearly, lunar monthly, and daily. Use of this large acoustic data set provided novel insights into temporal patterns in acoustic activity throughout entire seasonal, lunar,

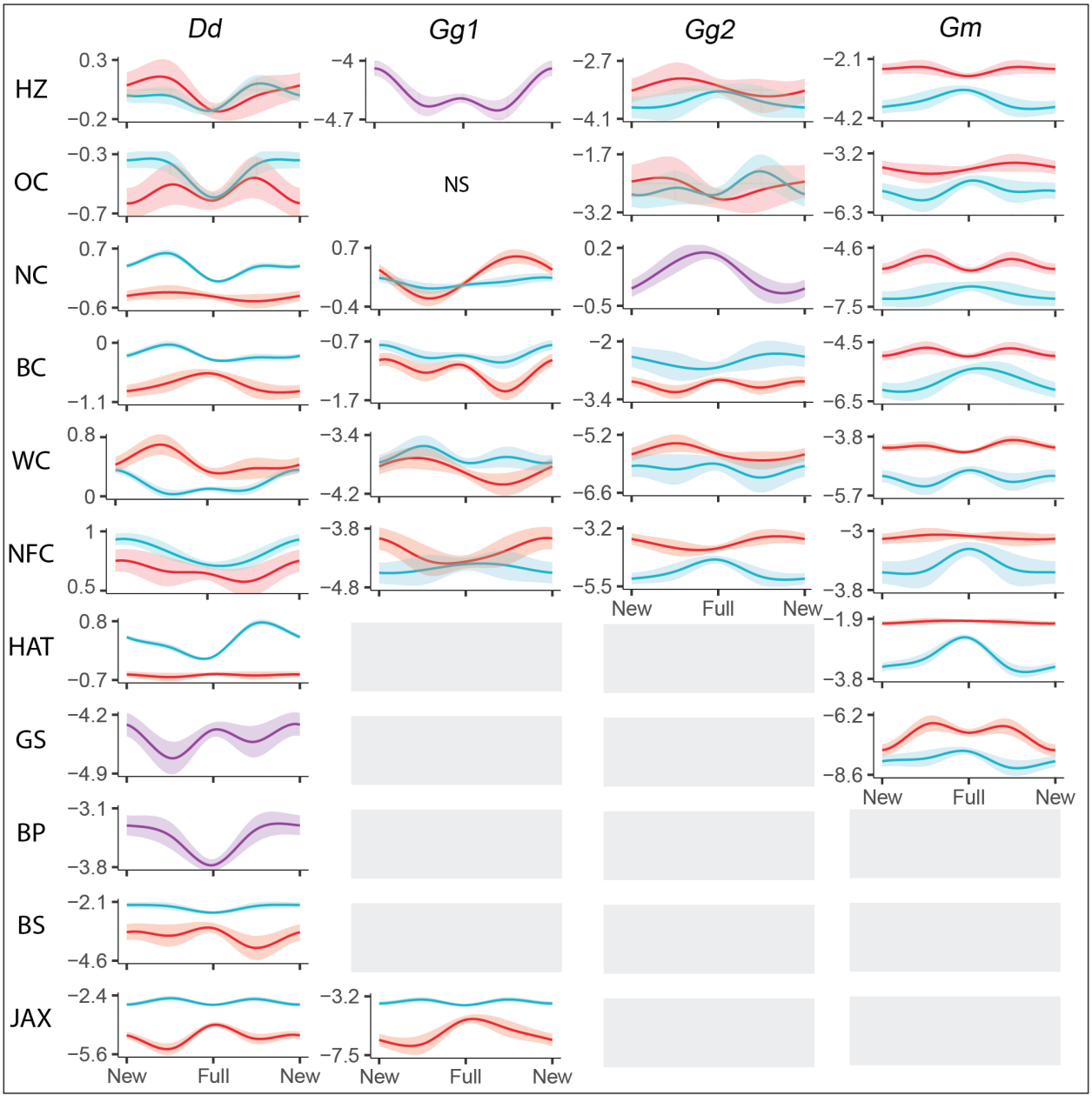

Fig. 5. Partial fits of moon phase (MPh) for the dolphin species. *Y*-axes give values of s(MPh); other terms were held constant at their mean values. Shaded regions: 95% CIs; gray blocks: no model due to low presence and/or poor performance. Plots showing a single curve (purple) depict the lunar pattern in the absence of significant interactions; plots with 2 curves depict the lunar patterns in the daytime (red) and nighttime (blue) when there was a significant interaction between MPh and normalized time of day (NT). Site and species abbreviations as in Fig. 1, Table 1

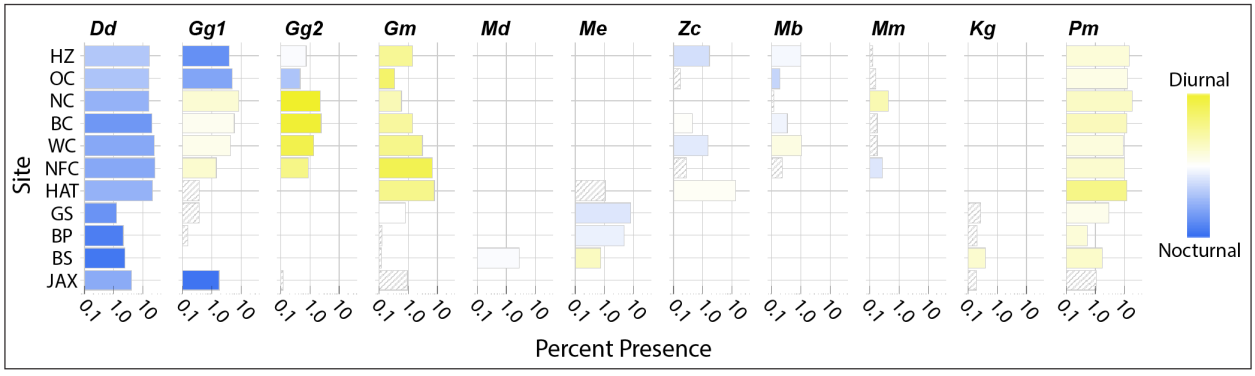

Fig. 6. Partitioning of acoustic presence between day and night. Bar length gives presence bins per thousand effort bins; note that the *x*-axis is in log scale. White bars indicate an even 50/50 split; bright yellow: 100% of presence occurring in the daytime; dark blue: 100% of presence occurring in the nighttime. Gray fill: normalized time of day was not significant; stripes: no model due to insufficient presence or poor model performance. Site and species abbreviations as in Fig. 1, Table 1

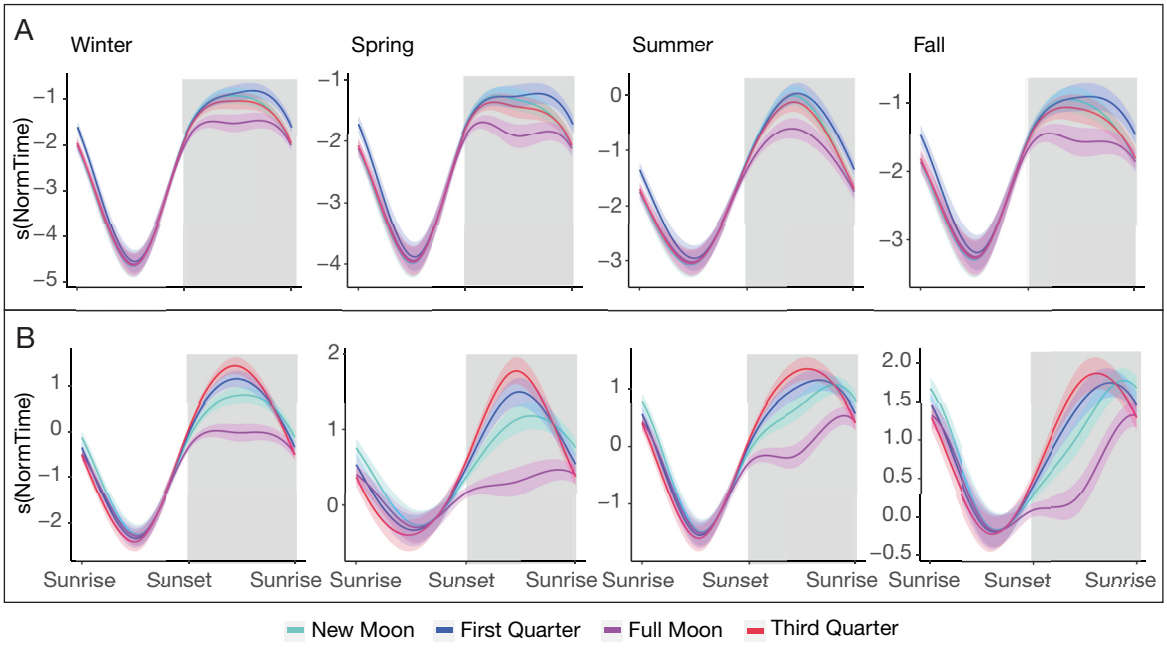

Fig. 7. Diel activity patterns for short-beaked common dolphins at (A) Oceanographer's Canyon, and (B) Cape Hatteras. Impacts of the lunar cycle differ between sites and throughout the year. Each panel represents the interaction between normalized time of day (NT) and day-of-year (DOY) at a different point in the seasonal cycle; colors in each panel show the interaction between NT and moon phase; shaded regions indicate nighttime

and diel cycles, and thus we can address some of the knowledge gaps associated with the visual survey data for this region, which is largely focused on summer months. Most of the species in this analysis were present primarily from HAT northwards; only 3 of the 10 species analyzed (*Md*, *Me*, and *Kg*) mainly occupied the southern sites. The acoustic monitoring sites used here are point sampling locations with limited monitoring volumes, so species that were apparently absent from one of our sites may indeed be present at that latitude, either further inshore or offshore, and thus not captured by our sampling design. But within each instrument's recording radius (~2 km; Hildebrand et al. 2015, Frasier et al. 2016), the ubiquitous use of echolocation for foraging, environmental sensing, and communication makes it a good proxy for detecting odontocete species occurrence. (Cohen et al. 2022) showed good alignment between the distributions of visually detected and acoustically detected animals for species that are amenable to visual surveys, while acoustic methods have been shown to detect higher levels of presence of cryptic species

than visual surveys (Yack et al. 2010). The regional differences in species distributions shown here are also consistent with previous findings that dolphin species exhibit preferences for particular temperature and salinity ranges (Fullard et al. 2000, Doksæter et al. 2008, Roberts et al. 2016).

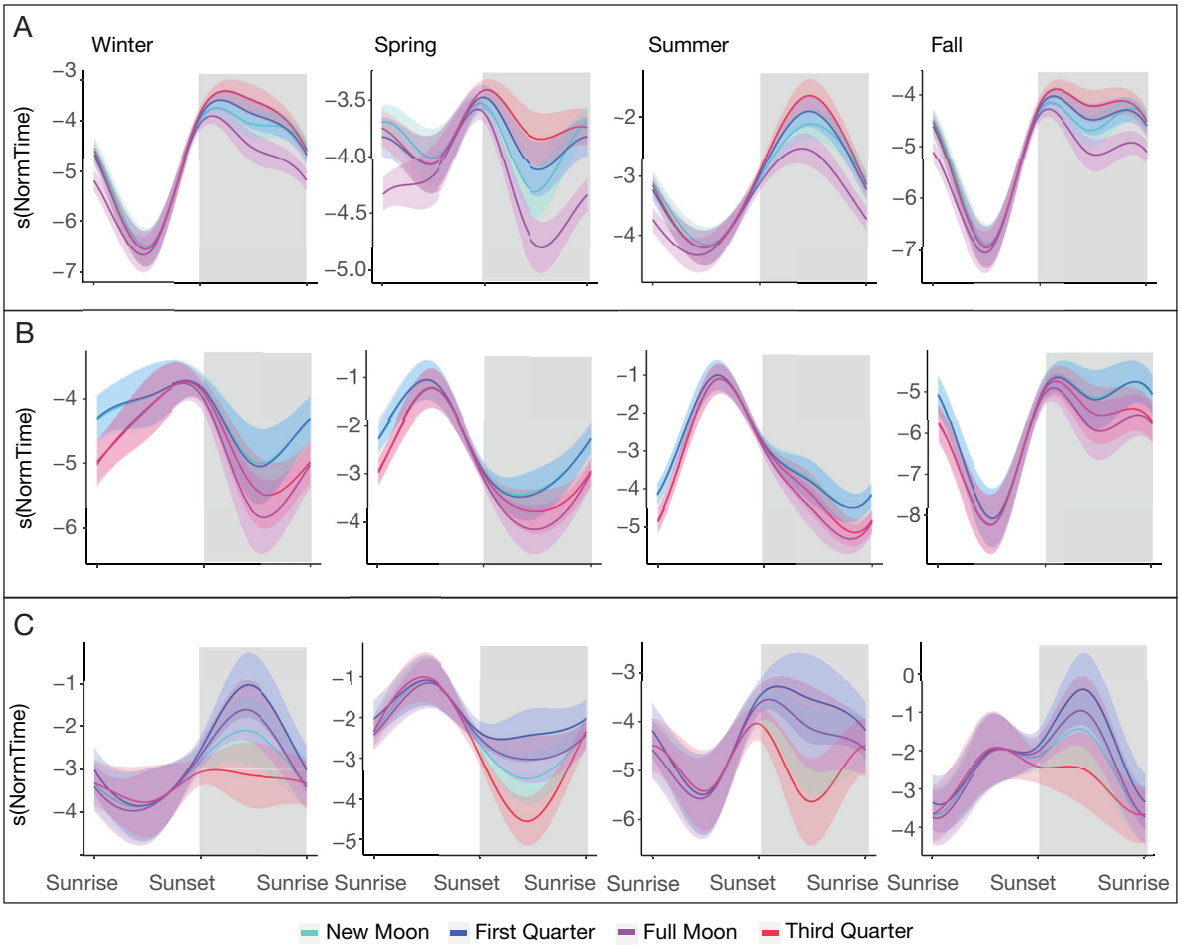

Fig. 8. Diel activity patterns for the Risso's dolphin click types *Gg1* and *Gg2* at Babylon Canyon (BC) and Norfolk Canyon (NFC). Panels, colors, and shading as in Fig. 7. (A) At BC, *Gg1* was primarily nocturnal, while (B) *Gg2* was often diurnal. (C) The diel activity patterns of *Gg2* at NFC showed substantial lunar modulation. Each panel represents the interaction between normalized time of day (NT) and day-of-year at a different point in the seasonal cycle; colors in each panel show the interaction between NT and moon phase; shaded regions indicate nighttime

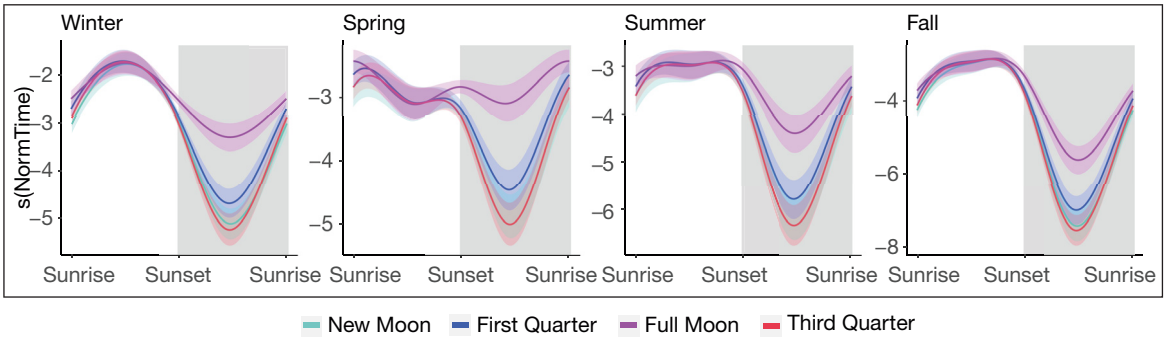

Fig. 9. Diel activity patterns for short-finned pilot whales at Cate Hatteras. Panels, colors, and shading as in Fig. 7. The impact of the lunar cycle can be seen to vary throughout the year. Each panel represents the interaction between normalized time of day (NT) and day-of-year at a different point in the seasonal cycle; colors in each panel show the interaction between NT and moon phase; shaded regions indicate nighttime

The GEEGAM framework generally performed well for characterizing relationships between species presence and the temporal covariates considered here, although the models clearly struggled in cases of very low species presence (Table 2). Of the models presented here, even those with performance approaching our model fit threshold (≥60% binned residuals within the 95% confidence intervals) were generally successful in describing seasonal patterns that were consistent with those suggested by histograms of presence binned with monthly resolution; their success with describing lunar and diel patterns was more mixed. Models for deep divers generally had lower McFadden's pseudo-R^2 values, which, in combination with lower retention of the MPh term and more instances of wide and overlapping confidence intervals, seems to suggest lesser importance of these temporal drivers for deep divers than for shallow and intermediate divers.

One challenge of working with this modeling framework was the scarcity of existing open-source software libraries for fitting, evaluating, or plotting GEEGAMs. This may act as a barrier to the wider adoption of GEEGAMs in ecological applications, despite the strength of these models over GAMs when it comes to working with serially autocorrelated data. The logistic nature of our models presented another challenge in terms of evaluating model fit. Typical residual-vs.-fitted value plots and R^2 values are not well-suited to logistic regression models, and some pseudo-R^2 metrics intended for logistic regression perform poorly in cases of low presence and low overall predicted probabilities, which was the case for most of our models.

4.1. Temporal pattern variations

We found substantial interspecific variability, as well as intraspecific regional variation, in seasonal, lunar, and diel patterns in odontocete acoustic activity. Such patterns in odontocete presence and acoustic activity are generally thought to be driven largely by the availability of preferred prey species, dictated by oceanographic conditions (Kampa 1975, Legendre 1990, Martin & Richards 2001, Biktashev et al. 2003, Last et al. 2016, Della Penna & Gaube 2020). This assumption is particularly relevant to this analysis since echolocation clicks were used as the indication of presence, and biosonar is known to be the primary mode of sensing prey for all odontocete species (Au 1993, Berta et al. 1999). Indeed, some of the patterns observed here are well-aligned with current knowledge of foraging ecology for these species. Echolocation may also be used for communicatory purposes (Watkins & Schevill 1977, Nemiroff & Whitehead 2009, Clausen et al. 2011), but a manual review of the raw data showed that the overwhelming majority of clicks detected on our devices were regular echolocation trains believed to be used primarily in foraging. Interspecies differences in site occupancy or activity patterns may be a means of minimizing competitive interactions (Conners et al. 2015, Gao et al. 2020, Iwahara et al. 2020, Lear et al. 2021). Intraspecies variability in lunar and diel preferences may be a response to seasonally and/or regionally variable prey behavior and density and may also be an indication of prey switching.

4.2. Beaked whales and deep-diving delphinids are spatially and temporally separated

Each beaked whale species exhibited a specific geographic locus of highest presence, distinct from the other species. However, differing seasonal peaks in presence did little to mitigate temporal overlap between *Zc* and *Mb* at shared sites in the north, and between *Md* and *Me* at site BS in the south. Apparent temporal separation was noted between the 2 deep-diving dolphin species, *Gg* and *Gm*: from NFC northwards, the seasonal peaks in *Gm* presence fell generally during the seasonal dips in *Gg* presence (also during the seasonal absence of *Dd* at most of these sites). In this case, differences in season of peak presence seemed to more effectively mitigate co-occurrence, as indicated by low coefficient of overlap values (Table 4). These differences in Δ values for beaked whales and dolphins result from a combination of 2 things: (1) less temporal separation between seasons of peak presence for beaked whales versus dolphins (Figs. 3 & 4), and (2) less pronounced modulation in presence over the seasonal cycle for beaked whales versus dolphins (apparent from histograms of presence binned across the seasonal cycle). The non-overlapping pattern of beaked whale site occupancy is consistent with what has been previously reported from this region and others (Baumann-Pickering et al. 2014, Stanistreet et al. 2017, Kowarski et al. 2018, Rice et al. 2021), although few works have identified habitat partitioning among dolphin species (Bearzi 2005).

This spatiotemporal separation of site occupancy may be a means of minimizing direct competition for similar prey through behavioral differentiation and may also reveal subtle differences in realized niche between

species with highly overlapping fundamental niches. Consideration of biotic and abiotic oceanographic conditions experienced at each of these sites through time may shed some light on the prey species and/or life stages of prey that are likely available, and the drivers of habitat selection for these odontocete species.

4.3. Possible evidence of seasonal north–south and onshore–offshore movements

The latitudinal shifts in seasonal peak presence for both *Gg* click types suggests seasonal migrations between the central and northern sites; the seasonal bimodality at NC may arise from the movement of animals through this site on their way to and from their spring and fall habitats. For *Gm*, we can similarly speculate about seasonal movements between north-central spring grounds (NFC, WC, BC) and either central (HAT, GS) or northern (OC, HZ) winter grounds. As noted in Cohen et al. (2022), the click type identified as *Gm* exhibits an upwards frequency shift at HZ; this could potentially be indicative of acoustic differentiation between distinct populations, which may overlap at the mid-Atlantic Bight sites. The low predicted presence of both *Gg* and *Dd* at all our sites in the winter and fall, respectively, begs the question of what constitutes their cool-weather habitat in this region. One explanation for the absence of these species at all our sites during a portion of the year could be onshore–offshore movements that take them out of the sensing range of our shelf-break-situated instruments. Zonal movements have been previously observed for dolphins on both seasonal and diel cycles (Perrin et al. 1979, Elwen et al. 2006). A study incorporating sensors deployed along an onshore–offshore gradient could help address this knowledge gap.

4.4. Lunar and diel cycles differentially impact species according to their diving ecology

Variability in lunar and diel cycles was observed across sites and seasons for many of the species, although consistent and ecologically coherent patterns were only apparent for the dolphin species. Diel and lunar cycles in odontocete behavior are generally thought to be driven by light-mediated changes in prey depth distributions (Kampa 1975, Last et al. 2016) and the energetic costs of, or physiological limitations on, foraging in different depth layers. Such variability in diel and lunar activity patterns may indicate adaptability to fine-scale temporal and spatial differences in prey fields. For example, Abecassis et al. (2015) and Copeland et al. (2019) both reported sub-daily and daily scale foraging responsiveness of *Gm* to changes in the micronekton scattering layers, which constitute prey for the whale's own forage species. Consideration of differences in prey fields and oceanographic conditions across our sites may provide more meaningful insights into the drivers of this apparent behavioral plasticity.

Our findings of primarily nocturnal and crepuscular activity for *Gg1* are consistent with the current understanding of this species' foraging ecology, while the diurnal occurrence of the *Gg2* click type was surprising. *Gg* represent something of an intermediate between common dolphins and pilot whales in terms of foraging ecology. *Gg* forage in the upper 200 m during the night but are also known to undertake deep foraging dives during the daytime and around dusk to access prey below 400 m, and they meet scattering layers on their ascent (Benoit-Bird et al. 2019, Visser et al. 2021). They prey almost exclusively on cephalopods (Clarke & Pascoe 1985, Luna et al. 2022). We speculate that *Gg1* may be primarily associated with nighttime foraging at epipelagic depths, while *Gg2* may correspond to different foraging strategies or behavioral states. Another possible explanation is that the 2 click types correspond to distinct *Gg* populations with different foraging strategies, as suggested previously for the 2 distinct Pacific white-sided dolphin click types (Soldevilla et al. 2010b); however, this seems less likely given the spatial and seasonal co-occurrence of the 2 *Gg* click types.

The deep divers considered here exhibited a variety of lunar and diel patterns in acoustic activity, but no well-defined or consistent light–dark preferences were apparent either across species or within species for those modeled at multiple sites. Limited previous reports of diel and lunar patterns exist for a few of these species (Aoki et al. 2007, Henderson et al. 2016, Merkens et al. 2019, Barlow et al. 2020), but more work is needed to understand the drivers of the substantial variability in lunar and diel activity patterns observed here.

4.5. Lunar illumination modulates dolphin diel activity patterns

For *Gm* and *Dd*, observed lunar preferences were complementary to their respective diel patterns in terms of apparent light preferences and well-aligned with each species' foraging ecology. This suggests that the influence of lunar illumination on the depth

distribution of prey species, as opposed to an endogenous circadian rhythm, drives these observed lunar activity cycles. *Dd* exhibited highly consistent nocturnal activity patterns across sites and seasons and preferred darker nighttime conditions, with reduced nighttime acoustic activity around the full moon; daytime lunar patterns were variable between sites. Extremely limited work suggests that this species is a shallow diver, capable of attaining maximum depths of about 260 m (Stewart 2018). Offshore populations of *Dd* are known to forage on mesopelagic fish and, to a much lesser extent, squid (Pusineri et al. 2007, Doksæter et al. 2008), and primarily forage at night (Henderson et al. 2012). Presumably, these dolphins can only access such deep-dwelling prey species when they undergo nocturnal vertical migration into the epipelagic zone, a behavior that is suppressed by intense lunar illumination around the full moon (Last et al. 2016). The *Dd* diel and lunar patterns evident in this analysis are in keeping with nocturnal foraging on diel vertical migrators when they are most abundant in the surface waters.

Gm, on the other hand, are known to be deep divers capable of accessing prey at depths >1000 m (Aguilar Soto et al. 2008, Quick et al. 2017). Aguilar Soto et al. (2008) and Baird et al. (2003) both reported fewer but deeper dives during the day and a higher rate of diving to somewhat shallower depths at night. Owen et al. (2019) observed that during the full moon, nighttime deep dives of *Gm* were deeper and longer, although there was a reduction in the proportion of nighttime dives, whereas there were no changes in mean depth or duration of daytime deep dives. At HAT, the site with the highest acoustic presence of *Gm*, we observed a primarily diurnal pattern in acoustic activity, and an increase in nighttime acoustic activity around the full moon, with no meaningful changes in daytime acoustic activity over the course of the lunar cycle. At the northern sites, *Gm* were primarily crepuscular. This may indicate that pilot whales at HAT are targeting different prey than at the northern sites, which would not be surprising given the oceanographic differences between HAT and the northern sites, particularly in terms of vicinity to and influence of the Gulf Stream.

Previous work has demonstrated the importance of lunar influences on *Gg* foraging in southern California, with reduced acoustic activity around the full moon and more nighttime echolocation prior to moonrise than while the moon was present in the night sky or after moonset (Simonis 2017). In this analysis, *Gg* lunar patterns were highly variable across sites and between the 2 click types analyzed. This may suggest ocean basin differences in *Gg* populations, optimization of foraging strategies based on site-varying prey fields in our region, or both. It may also suggest that the lunar patterns exhibited by *Gg* are externally forced, similar to what we observed here for *Dd* and *Gm*, as endogenous circadian cycles would not be expected to vary by site for a species believed to traverse the entire region.

The data presented here demonstrate spatial and temporal separation of potentially competitive odontocete species in the western North Atlantic. Altogether, at temporal scales finer than seasonal, the extreme deep divers (beaked whales, *Pm*, *Kg*) seemed less affected by external temporal covariates than the delphinids, possibly be cause of specialized foraging in the presumably much less dynamic deep-sea environment. The variable temporal activity patterns presented here may illustrate behavioral approaches to minimizing direct prey competition among closely related species and provide new insights into the habitat use, behavioral plasticity, and foraging patterns of odontocete species.

Data availability. The data underlying this analysis are publicly available at https://datadryad.org (doi:10.6076/D1WS32).

Acknowledgements. This project used data collected through collaborations between the Scripps Institution of Oceanography and both the National Oceanic and Atmospheric Administration (NOAA) and the US Navy. Sofie Van Parijs and Danielle Cholewiak of NOAA Northeast Fisheries Science Center (NEFSC), Joel Bell of Naval Facilities Engineering Command (NAVFAC) Atlantic, Michael Richlen of HDR, and Andrew Read (Duke University) contributed greatly to project support and sampling design development. Many thanks to Eric Matzen of NEFSC, and Drexel 'Stormy' Harrington, Drex Harrington, and Bev Harrington of the 'Tiki XIV' for fieldwork support enabling instrument deployment and recovery. Members of the Whale Acoustics Laboratory, the Scripps Acoustic Ecology Lab, and the Scripps Machine Listening Lab, all at the Scripps Institution of Oceanography, contributed to this project at all stages: thanks to Bruce Thayre, John Hurwitz, Jennifer Trickey, and Ryan Griswold for acoustic device development, testing, deployment, and recovery; to Erin O'Neill for acoustic data pre-processing and quality control; and to Natalie Posdaljian and Morgan Ziegenhorn for collaboration on development of the statistical methods. Funding was provided by HDR MSA 1000300000780 (J.A.H.), Duke University–subcontract number 283-0280 Duke to UC (J.A.H.), and NOAA NEFSC-CIMEC Award NA10OAR4320156 (J.A.H.).

LITERATURE CITED

Abecassis M, Polovina J, Baird RW, Copeland A and others (2015) Characterizing a foraging hotspot for short-finned pilot whales and Blainville's beaked whales located off the west side of Hawai'i island by using tagging and oceanographic data. PLOS ONE 10:e0142628

Aguilar Soto N, Johnson MP, Madsen PT, Díaz F, Domínguez I, Brito A, Tyack P (2008) Cheetahs of the deep sea: deep foraging sprints in short-finned pilot whales off Tenerife (Canary Islands). J Anim Ecol 77:936–947

Aoki K, Amano M, Yoshioka M, Mori K, Tokuda D, Miyazaki N (2007) Diel diving behavior of sperm whales off Japan. Mar Ecol Prog Ser 349:277–287

Arranz P, de Soto NA, Madsen PT, Brito A, Bordes F, Johnson MP (2011) Following a foraging fish-finder: diel habitat use of Blainville's beaked whales revealed by echolocation. PLOS ONE 6:e28353

Au WWL (1993) The sonar of dolphins. Springer Verlag, New York, NY

Baird RW, McSweeney DJ, Heithaus MR, Marshall GJ (2003) Short-finned pilot whale deep diving behavior: deep feeders and daytime socialites. In: 15th Biennial conference on the biology of marine mammals. Greensboro, NC (Abstract)

Barlow J, Schorr GS, Falcone EA, Moretti D (2020) Variation in dive behavior of Cuvier's beaked whales with seafloor depth, time-of-day, and lunar illumination. Mar Ecol Prog Ser 644:199–214

Baumann-Pickering S, Roch MA, Brownell RL, Simonis AE and others (2014) Spatio-temporal patterns of beaked whale echolocation signals in the North Pacific. PLOS ONE 9:e86072

Baumann-Pickering S, Roch MA, Wiggins SM, Schnitzler HU, Hildebrand JA (2015) Acoustic behavior of melon-headed whales varies on a diel cycle. Behav Ecol Sociobiol 69:1553–1563

Bearzi M (2005) Habitat partitioning by three species of dolphins in Santa Monica Bay, California. Bull South Calif Acad Sci 104:113–124

Becker EA, Forney KA, Foley DG, Smith RC, Moore TJ, Barlow J (2014) Predicting seasonal density patterns of California cetaceans based on habitat models. Endang Species Res 23:1–22

Benjamins S, van Geel N, Hastie G, Elliott J, Wilson B (2017) Harbour porpoise distribution can vary at small spatiotemporal scales in energetic habitats. Deep Sea Res II 141:191–202

Benoit-Bird KJ, Southall BL, Moline MA (2019) Dynamic foraging by Risso's dolphins revealed in four dimensions. Mar Ecol Prog Ser 632:221–234

Berta A, Sumich JL, Kovacs KM (1999) Marine mammals: evolutionary biology. Academic Press, Cambridge, MA

Best BD, Halpin PN, Read AJ, Fujioka E and others (2012) Online cetacean habitat modeling system for the US East Coast and Gulf of Mexico. Endang Species Res 18:1–15

Biktashev VN, Brindley J, Horwood JW (2003) Phytoplankton blooms and fish recruitment rate. J Plankton Res 25: 21–33

Bower AS, Rossby HT, Lillibridge JL (1985) The Gulf Stream — Barrier or blender? J Phys Oceanogr 15: 24–32

Campos-Cerqueira M, Aide TM (2016) Improving distribution data of threatened species by combining acoustic monitoring and occupancy modelling. Methods Ecol Evol 7:1340–1348

Cascão I, Lammers MO, Prieto R, Santos RS, Silva MA (2020) Temporal patterns in acoustic presence and foraging activity of oceanic dolphins at seamounts in the Azores. Sci Rep 10:3610

Cavender-Bares KK, Karl DM, Chisholm SW (2001) Nutrient gradients in the western North Atlantic Ocean: relationship to microbial community structure and comparison to patterns in the Pacific Ocean. Deep Sea Res I 48: 2373–2395

Clarke MR, Pascoe PL (1985) The stomach contents of a Risso's dolphin (*Grampus griseus*) stranded at Thurlestone, South Devon. J Mar Biol Assoc UK 65:663–665

Clausen KT, Wahlberg M, Beedholm K, Deruiter S, Madsen PT (2011) Click communication in harbour porpoises *Phocoena phocoena*. Bioacoustics 20:1–28

Cohen J (1988) Statistical power analysis for the behavioral sciences, 2nd edn. Lawrence Erlbaum Associates, Mahwah, NJ

Cohen RE, Frasier KE, Baumann-Pickering S, Wiggins SM, Rafter MA, Baggett LM, Hildebrand JA (2022) Identification of western North Atlantic odontocete echolocation click types using machine learning and spatiotemporal correlates. PLOS ONE 17:e0264988

Conners MG, Hazen EL, Costa DP, Shaffer SA (2015) Shadowed by scale: subtle behavioral niche partitioning in two sympatric, tropical breeding albatross species. Mov Ecol 3:28

Copeland AM, Au WLW, Polovina J (2019) Influences of temporal changes in pelagic scattering layers on short-finned pilot whales behavior. Oceanogr Fish Open Access J 9:555758

Davis RW, Worthy GAJ, Würsig B, Lynn SK, Townsend FI (1996) Diving behavior and at sea movements of an Atlantic spotted dolphin in the Gulf of Mexico. Mar Mamm Sci 12:569–581

Della Penna A, Gaube P (2020) Meoscale eddies structure mesopelagic communities. Front Mar Sci 7:454

Doksæter L, Olsen E, Nøttestad L, Fernö A (2008) Distribution and feeding ecology of dolphins along the Mid-Atlantic Ridge between Iceland and the Azores. Deep Sea Res II 55:243–253

Elwen S, Meÿer MA, Best PB, Kotze PGH, Thornton M, Swanson S (2006) Range and movements of female Heaviside's dolphins (*Cephalorhynchus heavisidii*), as determined by satellite-linked telemetry. J Mammal 87: 866–877

Forney KA, Becker EA, Foley DG, Barlow J, Oleson EM (2015) Habitat-based models of cetacean density and distribution in the central North Pacific. Endang Species Res 27:1–20

Frasier KE (2021) A machine learning pipeline for classification of cetacean echolocation clicks in large underwater acoustic datasets. PLOS Comput Biol 17:e1009613

Frasier KE, Wiggins SM, Harris D, Marques TA, Thomas L, Hildebrand JA (2016) Delphinid echolocation click detection probability on near-seafloor sensors. J Acoust Soc Am 140:1918–1930

Frasier KE, Garrison LP, Soldevilla MS, Wiggins SM, Hildebrand JA (2021) Cetacean distribution models based on visual and passive acoustic data. Sci Rep 11:8240

Fullard KJ, Early G, Heide-Jørgensen MP, Bloch D, Rosing-Asvid A, Amos W (2000) Population structure of long-finned pilot whales in the North Atlantic: A correlation with sea surface temperature? Mol Ecol 9:949–958

Gannier A (1999) Diel variations of the striped dolphin distribution off the French Riviera (northwestern Mediterranean Sea). Aquat Mamm 25:123–124

Gao VD, Morley-Fletcher S, Maccari S, Vitaterna MH, Turek FW (2020) Resource competition shapes biological rhythms and promotes temporal niche differentiation in a community simulation. Ecol Evol 10:11322–11334

Gaskin DE (1984) The harbor porpoise *Phocoena phocoena* (L.): regional populations, status, and information on direct and indirect catches. Rep Int Whaling Comm 34:569–586

Gatien MG (1976) A study in the Slope Water region south of Halifax. J Fish Res Board Can 33:2213–2217

Gelman A, Hill J (2006) Data analysis using regression and multilevel/hierarchical models. Cambridge University Press, Cambridge

Gibb R, Browning E, Glover-Kapfer P, Jones KE (2019) Emerging opportunities and challenges for passive acoustics in ecological assessment and monitoring. Methods Ecol Evol 10:169–185

Halekoh U, Højsgaard S, Yan J (2006) The R package geepack for generalized estimating equations. J Stat Softw 15:1–11

Hamazaki T (2002) Spatiotemporal prediction models of cetacean habitats in the mid-western North Atlantic Ocean (from Cape Hatteras, North Carolina, USA to Nova Scotia, Canada). Mar Mamm Sci 18:920–939

Hastie TJ, Tibshirani RJ (1986) Generalized additive models. Stat Sci 1:297–318

Hastie GD, Wilson B, Wilson LJ, Parsons KM, Thompson PM (2004) Functional mechanisms underlying cetacean distribution patterns: hotspots for bottlenose dolphins are linked to foraging. Mar Biol 144:397–403

Henderson EE, Hildebrand JA, Smith MH, Falcone EA (2012) The behavioral context of common dolphin (*Delphinus* sp.) vocalizations. Mar Mamm Sci 28:439–460

Henderson EE, Martin SW, Manzano-Roth R, Matsuyama BM (2016) Occurrence and habitat use of foraging Blainville's beaked whales (*Meoplodon densirostris*) on a US Navy range in Hawaii. Aquat Mamm 42:549–562

Hildebrand JA, Baumann-Pickering S, Frasier KE, Trickey JS and others (2015) Passive acoustic monitoring of beaked whale densities in the Gulf of Mexico. Sci Rep 5:16343

Hildebrand JA, Frasier KE, Baumann-Pickering S, Wiggins SM and others (2019) Assessing seasonality and density from passive acoustic monitoring of signals presumed to be from pygmy and dwarf sperm whales in the Gulf of Mexico. Front Mar Sci 6:66

Hodge LEW, Baumann-Pickering S, Hildebrand JA, Bell JT and others (2018) Heard but not seen: occurrence of *Kogia* spp. along the western North Atlantic shelf break. Mar Mamm Sci 34:1141–1153

Iwahara Y, Shirakawa H, Miyashita K, Mitani Y (2020) Spatial niche partitioning among three small cetaceans in the eastern coastal area of Hokkaido, Japan. Mar Ecol Prog Ser 637:209–223

Kampa EM (1975) Observations of a sonic-scattering layer during the total solar eclipse 30 June, 1973. Deep-Sea Res Oceanogr Abstr 22:417–420

Kowarski K, Delarue J, Martin B, O'Brien J, Meade R, Cadhla O, Berrow S (2018) Signals from the deep: spatial and temporal acoustic occurrence of beaked whales off western Ireland. PLOS ONE 13:e0199431

Kowarski KA, Martin SB, Maxner EE, Lawrence CB, Delarue JJY, Miksis-Olds JL (2023) Cetacean acoustic occurrence on the US Atlantic Outer Continental Shelf from 2017 to 2020. Mar Mamm Sci 39:175–199

Last KS, Hobbs L, Berge J, Brierley AS, Cottier F (2016) Moonlight drives ocean-scale mass vertical migration of zooplankton during the Arctic winter. Curr Biol 26: 244–251

Lear KO, Whitney NM, Morris JJ, Gleiss AC (2021) Temporal niche partitioning as a novel mechanism promoting co-existence of sympatric predators in marine systems. Proc R Soc B 288:20210816

Legendre L (1990) The significance of microalgal blooms for fisheries and for the export of particulate organic carbon in oceans. J Plankton Res 12:681–699

Liang KY, Zeger SL (1986) Longitudinal data analysis using generalized linear models. Biometrika 73:13–22

Luna A, Sánchez P, Chicote C, Gazo M (2022) Cephalopods in the diet of Risso's dolphin (*Grampus griseus*) from the Mediterranean Sea: a review. Mar Mamm Sci 38: 725–741

Marques TA, Thomas L, Martin SW, Mellinger DK and others (2013) Estimating animal population density using passive acoustics. Biol Rev Camb Philos Soc 88: 287–309

Martin AP, Richards KJ (2001) Mechanisms for vertical nutrient transport within a North Atlantic mesoscale eddy. Deep Sea Res II 48:757–773

Matich P, Ault JS, Boucek RE, Bryan DR and others (2017) Ecological niche partitioning within a large predator guild in a nutrient-limited estuary. Limnol Oceanogr 62: 934–953

McFadden D (1973) Conditional logit analysis of qualitative choice behavior. In: Zarembka P (ed) Frontiers in econometrics. Academic Press, Cambridge, MA, p 105–142

McFadden D (1977) Quantitative methods for analyzing travel behaviour of individuals: some recent developments. Cowles Foundation Discussion Papers No. 474. Yale University, New Haven, CT

McLellan HJ (1957) On the distinctness and origin of the slope water off the Scotian Shelf and its easterly flow south of the Grand Banks. J Fish Res Board Can 14: 213–239

Mellinger DK, Stafford KM, Moore SE, Dziak RP, Matsumoto H (2007) An overview of fixed passive acoustic observation methods for cetaceans. Oceanography 20: 36–45

Merkens KP, Simonis AE, Oleson EM (2019) Geographic and temporal patterns in the acoustic detection of sperm whales *Physeter macrocephalus* in the central and western North Pacific Ocean. Endang Species Res 39:115–133

Møhl B, Wahlberg M, Madsen PT, Miller LA, Surlykke A (2000) Sperm whale clicks: directionality and source level revisited. J Acoust Soc Am 107:638–648

Møller A, Jennions MD (2002) How much variance can be explained by ecologists and evolutionary biologists? Oecologia 132:492–500

Nemiroff L, Whitehead H (2009) Structural characteristics of pulsed calls of long-finned pilot whales *Globicephala melas*. Bioacoustics 19:67–92

New AL, Smeed DA, Czaja A, Blaker AT, Mecking JV, Mathews JP, Sanchez-Franks A (2021) Labrador Slope Water connects the subarctic with the Gulf Stream. Environ Res Lett 16:084019

Owen K, Andrews RD, Baird RW, Schorr GS, Webster DL (2019) Lunar cycles influence the diving behavior and habitat use of short-finned pilot whales around the main Hawaiian Islands. Mar Ecol Prog Ser 629:193–206

Pan W (2001) Akaike's information criterion in generalized estimating equations. Biometrics 57:120–125

Perrin WF, Evans WE, Holts DB (1979) Movements of pelagic dolphins (*Stenella* spp.) in the eastern tropical Pacific as indicated by results of tagging, with summary of tagging operations, 1969–76. NOAA Tech Rep NMFS-SSRF-737

Piatt JF, Methven DA (1992) Threshold foraging behavior of baleen whales. Mar Ecol Prog Ser 84:205–210
Picciulin M, Kéver L, Parmentier E, Bolgan M (2019) Listening to the unseen: passive acoustic monitoring reveals the presence of a cryptic fish species. Aquat Conserv 29: 202–210
Pirotta E, Matthiopoulos J, MacKenzie M, Scott-Hayward L, Rendell L (2011) Modelling sperm whale habitat preference: a novel approach combining transect and follow data. Mar Ecol Prog Ser 436:257–272
Pusineri C, Magnin V, Meynier L, Spitz J, Hassani S, Ridoux V (2007) Food and feeding ecology of the common dolphin (*Delphinus delphis*) in the oceanic Northeast Atlantic and comparison with its diet in neritic areas. Mar Mamm Sci 23:30–47
Quick NJ, Isojunno S, Sadykova D, Bowers M, Nowacek DP, Read AJ (2017) Hidden Markov models reveal complexity in the diving behaviour of short-finned pilot whales. Sci Rep 7:45765
Core Team (2021) R: a language and environment for statistical computing. R Foundation for Statistical Computing, Vienna. https://www.R-project.org/
Redfern JV, Ferguson MC, Becker EA, Hyrenbach KD and others (2006) Techniques for cetacean–habitat modeling. Mar Ecol Prog Ser 310:271–295
Rice A, Širović A, Trickey JS, Debich AJ and others (2021) Cetacean occurrence in the Gulf of Alaska from long-term passive acoustic monitoring. Mar Biol 168:72
Ridout MS, Linkie M (2009) Estimating overlap of daily activity patterns from camera trap data. J Agric Biol Environ Stat 14:322–337
Roberts JJ, Best BD, Mannocci L, Fujioka E and others (2016) Habitat-based cetacean density models for the US Atlantic and Gulf of Mexico. Sci Rep 6:22615
Simonis AE (2017) By the light of the moon: North Pacific dolphins optimize foraging with the lunar cycle. PhD dissertation, University of California, San Diego, CA
Simonis AE, Roch MA, Bailey B, Barlow J and others (2017) Lunar cycles affect common dolphin *Delphinus delphis* foraging in the Southern California Bight. Mar Ecol Prog Ser 577:221–235
Soldevilla MS, Henderson EE, Campbell GS, Wiggins SM, Hildebrand JA, Roch MA (2008) Classification of Risso's and Pacific white-sided dolphins using spectral properties of echolocation clicks. J Acoust Soc Am 124:609–624
Soldevilla MS, Wiggins SM, Hildebrand JA (2010a) Spatial and temporal patterns of Risso's dolphin echolocation in the Southern California Bight. J Acoust Soc Am 127: 124–132
Soldevilla MS, Wiggins SM, Hildebrand JA (2010b) Spatio-temporal comparison of Pacific white-sided dolphin echolocation click types. Aquat Biol 9:49–62
Soldevilla MS, Wiggins SM, Hildebrand JA, Oleson EM, Ferguson MC (2011) Risso's and Pacific white-sided dolphin habitat modeling from passive acoustic monitoring. Mar Ecol Prog Ser 423:247–260
Stanistreet JE, Nowacek DP, Baumann-Pickering S, Bell JT and others (2017) Using passive acoustic monitoring to document the distribution of beaked whale species in the western North Atlantic Ocean. Can J Fish Aquat Sci 74: 2098–2109
Stanistreet JE, Nowacek DP, Bell JT, Cholewiak DM and others (2018) Spatial and seasonal patterns in acoustic detections of sperm whales *Physeter macrocephalus* along the continental slope in the western North Atlantic Ocean. Endang Species Res 35:1–13
Stewart BS (2018) Diving behavior. In: Würsig B, Thewissen JGM, Kovacs KM (eds) Encyclopedia of marine mammals, 3rd edn. Academic Press, Cambridge, MA, p 262–267
Taylor AR, Schacke JH, Speakman TR, Castleberry SB, Chandler RB (2016) Factors related to common bottlenose dolphin (*Tursiops truncatus*) seasonal migration along South Carolina and Georgia coasts, USA. Anim Migr 3:14–26
Thieurmel B, Elmarhraoui A (2019) suncalc: compute sun position, sunlight phases, moon position and lunar phase. R package v.0.5.0. https://CRAN.R-project.org/package=suncalc
Thorne LH, Heywood EI, Hirtle NO (2022) Rapid restructuring of the odontocete community in an ocean warming hotspot. Glob Change Biol 28:6524–6540
Visser F, Keller OA, Oudejans MG, Nowacek DP, Kok ACM, Huisman J, Sterck EHM (2021) Risso's dolphins perform spin dives to target deep-dwelling prey. R Soc Open Sci 8:202320
Visser F, Oudejans MG, Keller OA, Madsen PT, Johnson M (2022) Sowerby's beaked whale biosonar and movement strategy indicate deep-sea foraging niche differentiation in mesoplodont whales. J Exp Biol 225:jeb243728
Wang W, Yan J (2021) Shape-restricted regression splines with R package splines2. J Data Sci 19:498–517
Wang S, Lin Y, Gifford S, Eveleth R, Cassar N (2018) Linking patterns of net community production and marine microbial community structure in the western North Atlantic. ISME J 12:2582–2595
Watkins WA, Schevill WE (1977) Sperm whale codas. J Acoust Soc Am 62:1485–1490
Wiggins SM, Hildebrand JA (2007) High-frequency acoustic recording package (HARP) for broad-band, long-term marine mammal monitoring. In: Symposium on underwater technology and workshop on scientific use of submarine cables and related technologies, 17–20 April 2007, Tokyo. IEEE, New York, NY, p 551–557
Woodworth PA, Schorr GS, Baird RW, Webster DL and others (2012) Eddies as offshore foraging grounds for melon-headed whales (*Peponocephala electra*). Mar Mamm Sci 28:638–647
Yack TM, Barlow J, Roch MA, Klinck H, Martin S, Mellinger DK, Gillespie D (2010) Comparison of beaked whale detection algorithms. Appl Acoust 71:1043–1049
Ziegenhorn MA, Hildebrand JA, Oleson EM, Baird RW, Wiggins SM, Baumann-Pickering S (2023) Odontocete spatial patterns and temporal drivers of detection at sites in the Hawaiian Islands. Ecol Evol 13:e9688

Editorial responsibility: Robert Suryan, Juneau, Alaska, USA
Reviewed by: F. M. van Beest, E. T. Griffiths, A. Andriolo, L. D. Williamson

Submitted: October 3, 2022
Accepted: August 2, 2023
Proofs received from author(s): September 5, 2023